

รายงานฉบับสมบูรณ์

โครงการ การศึกษาเชิงชีวเคมีและชีวพิสิกส์ของกลไกการออกฤทธิ์ที่ระดับ ไมเลกุลของโบรตินฆ่าแมลงจากแบจทีเรีย Bacillus thuringiensis

> Biochemical and Biophysical Studies on the Molecular Mechanism of Action of Becillus thuringiensis Insecticidal Proteins

> > โดย นายชนันท์ อังคุธแสมบัติ

30 พฤศจิกายน 2546

รายงานฉบับสมบูรณ์

โครงการ การศึกษาเชิงชีวเคมีและชีวฟิสิกส์ของกลไกการออกฤทธิ์ที่ระดับ โมเลกุลของโปรดีนฆ่าแมลงจากแบคทีเรีย Bacillus thuringiensis

> Biochemical and Biophysical Studies on the Molecular Mechanism of Action of *Bacillus thuringiensis* Insecticidal Proteins

ผู้วิจัย

นายชนันท์ อังศุธนสมบัติ

สังกัด

สถาบันอณูชีววิทยาและพันธุศาสตร์ มหาวิทยาลัยมหิดล

สนับสนุนโดยสำนักงานกองทุนสนับสนุนการวิจัย

Acknowledgements

I am grateful to Prof. Sakol Panyim, Prof. Jean-Louis Schwartz and Prof. Yechiel Shai for valuable comments, to Drs G. Katzenmeier, Chartchai Krittanai, Kusol Pootanakit and Panadda Boonserm for helpful discussion and to Somphob Leetacheewa, Umnaj Chanama, Somsri Sakdee, Chaweewan Shimwai and Anchalee Nirachanon for technical assistance. This work was supported in part by grant number BRG44-8-0008 from the Thailand Research Fund. Golden Jubilee Ph.D. research scholarships to Issara Sramala, Theeraporn Puntheeranurak, Walairat Pornwiroon and Yodsoi Kanintronkul are gratefully acknowledged.

Chanan Angsuthanasombat February 5, 2004 Project Code: RSA44-8-0008

Project Title:

การศึกษาเชิงชีวเคมีและชีวฟิสิกส์ของกลไกการออกฤทธิ์ที่ระดับโมเลกุลของโปรดีน สารพิษฆ่าแมลงจากแบคทีเรีย Bacillus thuringiensis

Biochemical and Biophysical Studies on the Molecular Mechanism of Action of Bacillus thuringiensis Insecticidal Proteins

Investigator: Chanan Angsuthanasombat, Ph.D.

Institute of Molecular Biology and Genetics,

Mahidol University

E-mail Address: stcas@mahidol.ac.th

Project Period: 3 years (December 1, 2000 - November 30, 2003)

Abstract

Bacillus thuringiensis Cry δ-endotoxins have been demonstrated to act by forming a lytic pore in midgut epithelial cell membranes of the susceptible insect larvae. Previously, we have employed single proline substitutions and demonstrated that α4 and α5 within the pore-forming domain of the 130-kDa Cry4Ba toxin are important determinants of toxicity against Aedes aegypti mosquito-larvae, likely being involved in membrane-pore formation. Further analysis by charged-to alanine scanning mutagenesis revealed a crucial role in toxin activity for the positively charged side chain of arginine-158 in helix 4. In this report, an analogous effect on larvicidal activity was also observed for Arg-136 in helix 4 of the 65-kDa dipteran-specific Cry11Aa toxin. Interestingly, further conversions of this critical arginine residue to the most conserved residue lysine also abolished the Cry11Aa wild-type activity. For Cry4Ba, we have further found that the larvicidal-inactive Arg-158 mutant toxins (R158A and R158K) showed a decrease in ion-channel conductance in planar lipid bilayers (PLBs), suggesting that this residue is conceivably involved in the passage of ions through the pore. Unrestrained molecular dynamics (MD) simulations were performed with a modelled pore comprising 6 copies of the Cry4Ba α 4- α 5 hairpin or its derivatives placed in solvated lipid membrane bilayers (POPC/water). The MD results suggested that mutations at the critical Arg-158 residue affect structural integrity of the toxin-induced pore. The \alpha1-\alpha5 fragment of Cry4Ba was shown to form cation-selective channels in PLBs, supporting that this fragment constitutes the region responsible for pore-forming activity of the toxin. Directed mutations within the loop linking $\alpha 4$ and $\alpha 5$ of Cry4Ba were also performed and revealed that Asn-166, Tyr-170 and Glu-171 play a crucial role in mosquito-larvicidal activity, especially polarity at position 166 and aromaticity at position 170. A crucial role in toxin activity was also revealed for the conserved aromatic residue at position 202 within the $\alpha 4$ - $\alpha 5$ loop of the Cry4Aa toxin. These results support the notion that an aromatic structure of the highly conserved tyrosine residue within the $\alpha 4$ - $\alpha 5$ loop is an essential prerequisite for toxic action of the Cry δ -endotoxins.

Keywords: Bacillus thuringiensis, δ-endotoxin, ion channel, larvicidal activity, mutagenesis

บทคัดย่อ

โปรตีนสารพิษจากแบคทีเรีย Bacillus thuringiensis สามารถฆ่าหนอนแมลงโดยทำให้เกิดรูรั่วที่ ผนังเยื่อหุ้มเชลล์บุกระเพาะ (midgut epithelial cell membranes) จากรายงานก่อนหน้านี้ เราได้อาศัย วิชีการเปลี่ยนแปลงยืนโดยการแทนที่ด้วยกรดอะมิโน proline พบว่า เกลียวอัลฟาที่ 4 และ 5 (α-helices 4 and 5) ซึ่งอยู่ในส่วนโครงสร้างที่เชื่อว่าทำหน้าที่รับผิดชอบในการสอดแทรกและการเกิดรูรั่วที่ ผนังแขื่อทุ้มเซลล์นั้น มีส่วนเกี่ยวข้องกับการออกฤทธิ์ฆ่าลูกน้ำยุงลาย (Aedes aegypt) ของโปรตีน Cry4Ba และเมื่อใช้วิธีการ charged-to alanine scanning mutagenesis เพื่อศึกษาบทบาทของกรดอะมี ในที่มีประจุในเกลียวอัลฟาที่ 4 พบว่า ความเป็นประจุของกรดอะมิโน arginine ที่ตำแหน่ง 158 นั้น มี ความสำคัญต่อความเป็นพิษของโปรดีนข่าลูกน้ำยุงดังกล่าว ในรายงานนี้ เมื่อศึกษาเพิ่มเติมได้พบ ความสำคัญต่อความเป็นพิษของประจุบวกในเกลียวอัลฟาที่ 4 ของโปรดีนฆ่าลูกน้ำยุง Cry11Aa เช่นกัน ส่วนสำหรับโปรตีน Cry4Ba นั้น เราพบว่า โปรตีนกลายพันธุ์ชนิด R158A และ R158K ซึ่งได้สูญเสีย ฤทธิ์ฆ่าลูกน้ำยุงนั้น ให้ค่าความนำไฟฟ้า (conductance) ที่เกิดจากรูอิออน (ion channels) บน planar lipid bilayers ลดลง จึงพอสรุปได้ว่า Arg-158 ในเกลียวอัลฟาที่ 4 มีส่วนเกี่ยวข้องโดยตรงกับการ ควบคุมอิออนที่ผ่านเข้าออกรูรั่วซึ่งเกิดจากโปรตีน Cry4Ba และจากข้อมูลของการศึกษาดังกล่าวนี้ จึง ทำให้สามารถสร้างแบบจำลองของรูรั่วในผนังรูรั่วใต้อย่างมีหลักฐานที่สนับสนุนได้โดยอาศัยวิชี SA/MD (Simulated Anneal / Molecular Dynamics) Simulations นอกจากนี้ พบว่าซิ้นส่วนโปรตีน Cry4Ba ที่ ประกอบด้วยเกลียวอัลฟาที่ 1 ถึง 5 สามารถทำให้เกิดรูอิออนบน planar lipid bilayers ได้ ซึ่งสามารถ สรุปได้ว่า α1-α5 เป็นส่วนที่รับผิดขอบในการสอดแทรกและการเกิดรูรั่วหรือรูอิออนที่ผนังแยื่อทุ้มเซลล์ และเมื่อศึกษาเพิ่มเดิมพบว่าความเป็นขั้ว (polarity) ที่ดำแหน่ง 166 และ ลักษณะเป็น aromatic ที่ ตำแหน่ง 170 ซึ่งอยู่บนส่วนต่อระหว่างเกลียวอัลฟาที่ 4 และ 5 (α4-α5 loop) ของโปรดีน Cry4Ba นั้นมี ความสำคัญต่อฤทธิ์ฆ่าลูกน้ำยุง นอกจากนี้ยังพบว่า ลักษณะ aromatic ของ Tyr-202 ซึ่งอยู่บน α4-α5 loop ของโปรดีน Cry4Aa มีความสำคัญต่อฤทธิ์ฆ่าลูกน้ำยุงเช่นกัน จึงสามารถสรุปใต้ว่า ลักษณะ aromatic ของ tyrosine ซึ่งเป็นดำแหน่งที่อนุรักษ์ที่อยู่บน α4-α5 loop นั้น มีความจำเป็นสำหรับการ ออกฤทธิ์ของ Cry δ-endotoxins

Introduction

Bacillus thuringiensis (Bt) has been used successfully as an alternative insecticide for biological control of disease vectors and other pests. During sporulation, different Bt strains produce larvicidal proteins in large quantities as cytoplasmic crystalline inclusions that are specifically toxic to a variety of dipteran, lepidopteran and coleopteran insect larvae [Aronson et al., 1986; Schnepf et al., 1998]. These parasporal crystalline inclusions are composed of one or more polypeptides of varying molecular mass that have been classified as Cry and/or Cyt δ-endotoxins according to the similarity of their deduced amino acid sequences [Hofte & Whiteley, 1989; Crickmore et al., 1998].

The general mechanism of gut epithelial cell disruption by the different Bt δ -endotoxins is evidenced to be the formation of lytic pores in the susceptible insect membrane [Knowles & Ellar, 1987]. When ingested by susceptible larvae, the inclusions are solubilised by the alkaline pH of the larval midgut and the protoxins are activated by gut proteases. It is believed that the activated toxins then bind to midgut epithelial cells via specific receptors, and insert into the microvillar membrane to form ion channels or leakage pores that cause cell swelling and eventually death by colloid-osmotic lysis [see Knowles, 1994 for reviews]. However, an entire characterisation at the molecular level of the pore-forming process mediated by these insecticidal proteins has not yet been obtained, although knowledge of how these insecticidal proteins function has increased substantially over the last decade.

The X-ray crystal structure of four different Cry toxins, Cry1Aa [Grochulski et al., 1995], Cry2Aa [Morse et al., 2001], Cry3Aa [Li et al., 1991] and Cry3Bb [Galitsky et al., 2001], reveals Cry proteins consisting of three distinct domains, and it is believed that each domain has a defined function including pore formation and receptor recognition. Domain I is a group of seven α -helices in which the central helix (α 5) is relatively hydrophobic and encircled by six other amphipathic helices. Domain II is the most variable part of the Cry toxin family and is composed of three anti-parallel β -sheets, each terminating in a surface-exposed loop. Domain III is a tightly packed β -sandwich of two anti-parallel sheets. It has been proposed that other members of this family will have the same overall tertiary structure since the core of the molecule including all the domain interfaces is built up from five amino acid sequence segments that are highly conserved throughout the entire Cry toxin family [Hofte & Whiteley, 1989; Li et al., 1991]. Structurally, it is immediately apparent that domain I is likely to be the transmembrane pore-forming apparatus. This domain contains five amphipathic helices (α 3, α 4, α 5, α 6 and α 7) that are theoretically long enough to span the bilayer lipid membrane and form a lytic pore [Li et al., 1991]. The possibility that this α -helical bundle in domain I is

essential for pore formation is supported by the feature that it is highly conserved in all Cry toxins [Hofte & Whiteley, 1989]. This notion is supported by several studies with truncated proteins corresponding to domain I of Cry1Ac [Walters et al., 1994], Cry3B2 [von Tersch et al., 1994] and Cry4Ba [Puntheeranuruk et al., 2001]

Molecular mechanism of membrane insertion and pore formation of the Cry toxins is now described in an 'umbrella' model [Knowles, 1994]. In this model, α4 and α5 form a helical hairpin to initiate membrane penetration upon specific receptor-binding in which structural rearrangement of the toxin occurs. After insertion of this hairpin, the other helices spread over the membrane surface followed by oligomerisation of the toxin [Gazit et al., 1998; Guereca & Bravo, 1999], resulting in formation of an initial tetrameric pore [Schwartz et al., 1997]. Currently, this model is supported by a number of experiments demonstrating a crucial role of α4 and α5 in membrane penetration and pore formation of different Cry toxins [Cummings et al., 1994; Schwartz et al., 1997; Gazit et al., 1998; Kumar & Aronson, 1999; Masson et al., 1999; Nunes-Valdes et al., 2001]. Recent studies have clearly demonstrated that the helix 4-loop-helix 5 hairpin is more active in membrane penetration than each of the isolated helices or their mixtures, consistent with its function as the membrane-inserted portion of the Cry toxins [Gerber & Shai, 2000].

Experimental Procedures

Construction of Mutant Toxin Plasmids

In vitro site-directed mutagenesis was performed using a Quickchange PCR-based mutagenesis kit (Stratagene) following the manufacturer's instructions. The full-length gene encoding the 65-kDa Cry11Aa toxin from the recombinant plasmid pBTC68A (a generous gift of Dr. Wattanalai Panbangred, Department of Biotechnology, Mahidol University, Thalland) was subcloned into the pMEx8 expression vector [Buttcher et al., 1990]. This resultant plasmid (pME4D) and the plasmid pMU388 containing the full-length *cry4Ba* toxin gene [Angsuthanasombat et al., 1987] were used as a template. Complementary mutagenic oligonucleotides were purchased from Prooligo Inc. (Singapore). All mutations were verified by DNA sequencing using an ABI prism 377 sequencer.

Toxin Expression and Characterisation

The wild type and mutant toxin genes were expressed in *E. coli* strain JM109 under control of the lacZ promoter. Cells were grown in LB medium plus 100 µg/ml of ampicillin until OD₆₀₀ reached 0.4-0.5 and incubation was continued for another 4 hrs after addition of IPTG to

TO STATE OF THE PARTY OF THE PA

a final concentration of 0.1 mM. E. coll cultures expressing each mutant as inclusion bodies were harvested by centrifugation, resuspended in 1 ml of distilled water and then disrupted in a French Pressure Cell at 16,000 psi. The crude lysates were centrifuged at 8,000g for 5 min and pellets obtained were washed 3 times in distilled water.

Protoxin inclusions (1 mg/ml) were solubilised in 50 mM Na₂CO₃, pH 9.0 and incubated at 37°C for 60 min as described previously [Angsuthanasombat et al., 1991]. After centrifugation for 10 min, the supernatants were analysed by SDS-15% (w/v) PAGE in comparison with the inclusion suspension. The solubilised protoxins were assessed for their proteolytic stability by digestion with TPCK treated) at a protoxin:trypsin ratio of 20:1 (w/w) for 16 hrs [Angsuthanasombat et al., 1991].

Toxin Purification via FPLC

E. coli cells expressing the 130-kDa Cry4Aa toxin as a soluble form or the 130-kDa Cry4Ba toxin as a cytoplasmic inclusion [Angsuthanasombat et al., 1987] were harvested by centrifugation, resuspended in distilled water and then disrupted in a French Pressure Cell at 16,000 psi. The crude lysates were centrifuged at 8,000 g for 10 minutes and the supernatant containing the soluble Cry4Aa protoxin was collected for further purification via a size-exclusion FPLC system (Superose 12 HR10, Amersham Biosciences Corp.) with a linear gradient of 10 mM sodium phosphate (NaH₂PO₄/ Na₂HPO₄) buffer, pH 9.0 at 0.5 mL/min. 1-mL fractions were collected and analysed by SDS-15% w/v polyacrylamide gel electrophoresis. The sediment inclusions obtained from disrupted cells expressing Cry4Ba was washed 3 times in distilled water. The inclusions (3 mg/mL) were solubilised in 10 mM sodium phosphate buffer, pH 9.0 at 37°C for 1 hour. Protein concentrations were determined by using a protein microassay (Bio-Rad), with bovine serum albumin fraction V as a standard.

The FPLC purified Cry4Aa protoxin and the solubilised Cry4Ba protoxin were further digested with trypsin (TPCK treated) at toxin:enzyme ratio of 20:1 (w/w). Trypsin-treated fractions were then purified on a size-exclusion FPLC system as described above.

Preparation of the α1-α5 Fragment

The α 1- α 5 polypeptides were expressed as inclusion bodies produced from the cloned α 1- α 5 cry4Ba gene segment in *E. coli.* They were partially purified as described earlier [Puntheeranuruk et al., 2001]. Since the α 1- α 5 fragment could not be solubilised in 50mM Na₂CO₃ buffer, pH 10.5, 50 mM Tris buffer, pH 8.8, was used. The solubilised protein was passed through a Centricon-10 (Millipore, Billerica, MA, USA) for concentrating before injection on a Superdex 200 FPLC column (Amersham Biosciences Corp.). The protein was detected in

- FREEDOM - EN BRIDGE DE LA

the void volume as an oligomer larger than 200 kDa. Prior to use, toxin solutions were vortexed and sonicated for about 1 minute to prevent aggregation.

Circular Dichroism (CD) Spectroscopy

CD spectra of the activated Cry4Ba toxin and the α 1- α 5 polypeptide were measured with a Jasco J-715 spectropolarimeter (Jasco Inc.). They were scanned between 185 and 280 nm at room temperature in a rectangular quartz cuvette with a 0.2-mm optical path length. CD measurements of Cry4Ba (n=3) and of the α 1- α 5 fragment (n=5) were taken at a rate of 20 nm/min. The concentrations of Cry4Ba and its α 1- α 5 fragment were 4.5 x 10⁻⁶ M and 3 x 10⁻³ M, respectively, as determined by far UV absorbance. Spectra were corrected for solvent baseline obtained under the same conditions. The molar circular dichroism Δ E at a given wavelength was calculated with the following formula: Δ E = (K x θ x M_r)/(c x N x d); where K is equal to 3298 x 10⁻⁴, θ is the measured ellipticity (in millidegrees), M_r is the molecular weight of the sample, c is the sample concentration (in g/ml), N is the number of peptide bonds of the sample and d is the optical path length of the sample cell (in cm). Reference spectra were obtained and scale calibration at 290 nm was performed with camphorsulfonic acid (CSA, Sigma-Aldrich Corp.) and the θ value of CSA was measured at the beginning of each experiment. The helical contents of the protein and its fragment were derived from their Δ E determined at 222 nm.

Planar Lipid Bilayers

Planar lipid bilayers were formed from the 7:2:1 (wt/wt) lipid mixture of PE, PC and Ch [Schwartz et al., 1993]. The final concentration was 25 mg/ml dissolved in decane. The 200-µm orifice drilled in a Delrin cup was pretreated with the same lipid mixture. The lipid bilayer was painted using a pre-pulled glass pipette dipped in the decane-lipid solution. Membranes had a typical capacitance of 150 to 250 pF and remained stable for several hours. Before toxin polypeptide reconstitution, the bilayer was monitored under non zero holding voltage conditions for more than 30 minutes to ensure that no contaminant-induced channel activity was present. Incorporation was performed by adding aliquots of the protein or its fragment directly to the cis chamber, which was stirred using a small magnetic flea until channel activity was observed. The insertion process was facilitated by applying a 100-mV holding potential across the bilayer. Channel activity was observed by the presence of distinct current jumps recorded during test voltage steps applied across the planar lipid bilayer. Activated Cry4Ba was used at concentrations between 150 and 300 nM, whereas the fragment concentration ranged from 4.3 to 430 nM. All experiments were performed at room temperature (25°C).

Single channel currents were recorded with an Axopatch-1D patch-clamp amplifier (Axon Instruments). Signals were digitized with a Digidata 1200 analog-to-digital converter using the Axoscope 8.0 software (both from Axon instruments) at a 50-kHz sampling frequency. They were low-pass filtered at 600 kHz and analysed on a personal computer using the Axoscope 8.0 software. The conductances (g) were determined as follows. In experiments where channel currents returned to the baseline, i.e. to the current level observed at any particular voltage in the absence of either the toxin or its fragment, the largest amplitude of the current steps observed from, or to, the baseline level was plotted against applied voltage (current-voltage relations, or I-V curves). In experiments where channel currents never returned to the baseline, i.e. in which at least one channel remained always open, the main channel current was obtained from the amplitude of the smallest current level observable for at least 50% of the duration of the recording. Finally, all observable current steps were measured for each voltage and the corresponding amplitudes were plotted versus voltage. For the three approaches described above, the conductances were then derived from the slopes of the linear regression lines to the data points. The conductances obtained for individual experiments were then averaged over the number of experiments performed under the same conditions. Results are expressed as means ± SEMs.

lon selectivity was measured under 450/150 mM KCI (cis/trans) asymmetrical conditions. The reversal potential (V_R) was obtained as the voltage for which the corresponding linear regression intersected the horizontal axis of the I-V curves, and compared to the value calculated for K⁺ according to Nernst equation. Channel selectivity for K⁺ over CI was derived from P_K / P_{CI} permeability ratios calculated using V_R values and the Goldman-Hodgkin-Katz equation (GHK) [Hille, 1992].

Molecular Dynamics Simulations

Coordinate of the putative transmembrane fragment (α4-α5) of Cry4Ba was obtained from the Cry4Ba homology model which has been constructed using the Cry3Aa crystal structure as a template. Models of pores formed by this helical hairpin were generated by simulated anneal/molecular dynamics (SA/MD) using Xplor V3.1 with the modified CHARMM PARAM 19 parameter set. Accessible surfaces of proteins were calculated by using Quanta V3.2 (Molecular Simulations). MD simulations on solvated model were performed using Gromacs 2.0 with the modified force field parameter set [Keer et al., 2000]. Display and examinations of model were carried out using Rasmol and Insight II (Molecular Simulations). Computations were performed om SGI Indigo, Cray 2000 or Linux/Intel Pentium II. Diagrams of structures were drawn using Molscript. Helix crossing angels, hilix-membrane tilting angle

and interhelical distances were determines with routines, written for Gromacs 2.0. Pore dimension and elestrostatic potential along axis were determined by using HOLE 2.0.

Mosquito-Larvicidal Assays

Larvicidal activity assays were performed as previously described [Angsuthanasombat et al., 1992] using 2-day old *A. aegypti* larvae reared from eggs supplied by the mosquito-rearing facility of the Institute of Molecular Biology and Genetics, Mahidol University, Thailand. About 500 larvae were reared in a container (22×30×10 cm deep) with approximately 3 I of distilled water supplemented with 0.2-0.3 g of rat diet pellets. In the assays, 1 ml of *E. coli* suspension (ca. 108 cells) was added to a 48-well microtitre plate (11.3 mm well diameter), with 10 larvae per well and a total of 100 larvae for each type of *E. coli* sample. *E. coli* cells containing the recombinant plasmid pMU388 and the pUC12 vector were used as positive and negative controls, respectively. Mortality was recorded after incubation for 24 hrs.

Results and Discussion

Specific Mutations in Helix 4 of the 65-kDa Cry11Aa Toxin

Based on a multiple-amino acid sequence alignment with the known crystal structures of Cry1Aa and Cry3Aa [Li et al., 1991; Grochulski et al., 1995] and the homology-based model of Cry4Ba, the predicted α4 and α5 were located within the pore-forming domain of Cry11Aa (see Fig. 1A). Charged amino acids in helix 4 have been shown to be critical for toxin activity [Kumar and Aronson, 1999; Masson et al., 1999]. To investigate a possible role for toxicity of charged and polar amino acids in α4 of Cry11Aa, the PCR-based mutagenesis strategy previously employed for Cry4Ba (as shown previously) was applied to obtain substitutions within Cry11Aa. We have initially generated eight Cry11Aa mutants in which three charged and five polar amino acids in helix 4 (Fig. 1B) were substituted with alanine. Most of the targeted residues, Tyr-125, Asn-128, Gin-135, Arg-136 and Gin-139, but not Lys-123, Ser-130 and Glu-141, are located at the hydrophilic surface (see Fig. 1C).

Expression of the mutant toxins in *E. coli* was controlled by the *tac* promoter. Upon addition of IPTG to mid-exponential phase cultures, all mutant toxins were predominantly produced as sedimentable inclusion bodies. Lysates were analysed by SDS-PAGE and immunoblotting, and the protein expression level of all mutant derivatives was found to be comparable to the wild type. The 65-kDa expressed mutant proteins specifically cross-reacted with antibodies raised against the Cry11Aa toxin (data not shown). However, two relatively

intense immuno-reactive bands of ca. 50 and ca. 35 kDa were detected in all mutant lysates indicating that the expressed mutant proteins are rather sensitive to proteolytic degradation.

The solubility of mutant protein inclusions in comparison to the wild-type inclusion was assessed by using carbonate buffer, pH 9.0. The amounts of the 65-kDa soluble proteins in the supernatant were compared with those of the proteins initially used in order to determine the percentage of protein solubilisation. All the mutant inclusions were found to be soluble to some extent in this buffer, giving less than 20% solubility which resembles closely the wild-type inclusions under similar conditions.

To determine the effect of mutations on toxicity, E. coli cells expressing each type of the mutant toxin were tested for their relative biological activity towards A. aegypti larvae. All assays were carried out in ten replicas for each sample and repeated three times; the mortality data recorded after a 24-hour incubation are shown in Fig. 2. Interestingly, only the R136A mutation resulted in a total loss of larvicidal activity while slanine substitutions at seven other positions (K123A, Y125A, M128A, S130A, Q135A, Q139A and E141A) still retained over 50% of the wild-type activity. When this critical arginine residue at position 136 was converted to aspartate, glutamine or even to the most conserved residue for positively charged side chain, as R136 mutants (R136D, R136Q and R136K) were shown to be nontoxic to mosquito larvae (see Fig. 2). These results could imply the requirement for the specific atructure of the positively charged side chain at this position. Perhaps Arg-136, which is likely to face the pore furner, could interact with an aqueous environment and thus somehow to face the pore furner, could interact with an aqueous environment and thus somehow stabilise the functional pore. However, the precise function of this residue remains to be stabilise the functional pore. However, the precise function of this residue remains to be

Protein expression levels and solubility of the inclusions suggested that the complete loss of toxicity observed for the R136A mutant is least likely to be caused by misfolding of the protein. Taken together, our results indicate that Arg-136 is a critical residue involved in Cry11As toxin activity. The data further support our previous findings that Arg-158 in α4 played a crucial role in toxicity of the 130-kDa Cry48a toxin since the single alanine substitution at this residue almost completely abolished its activity towards mosquito larvae. In addition, the subtraction to toxicity of both the lepidopteran-specific Cry1As and Cry1Ac toxins (Kumar & Important for toxicity of both the lepidopteran-specific Cry1As and Cry1Ac toxins (Klumar & Aronson, 1999; Masson et al., 1999). Two other negatively charged residues (Glu-129 and Asphonson, 1999; Masson et al., 1999). Two other negatively charged residues (Glu-129 and Asphonson, 1999; Nasson et al., 1999). Two other negatively charged residues (Glu-129 and Asphonson, 1999; Nasson et al., 1999). Two other negatively charged residues (Glu-129 and Asphonson, 1999; Nasson et al., 1999). Two other negatively charged residues (Glu-129 and Asphonson, 1999; Nasson et al., 1999).

.[6661 ,.ls 1e

Comparisons of structural models among Cry11Aa, Cry4Ba and Cry1Aa suggest that although Arg-136 of Cry11Aa is located on the opposite side of helix 4 relative to Arg-158 of Cry4Ba or Arg-131 of Cry1Aa, all these three critical residues are oriented on the side of helix 4 furthest away from helix 5 (see Fig. 3A). It should be noted that Arg-136 and Arg-158 in both of the dipteran-specific toxins, are situated near the C-terminal end of helix 4 while Arg-131 of the lepidopteran-specific Cry1Aa toxin is located furthest from the C-terminus of this helix (Fig. 3B). Differences in the location of these critical residues may conceivably reflect the diversity in the channel architecture for each group of insect-specific Cry toxins. Further studies are required to elucidate the role of these positively charged residues in helix 4 whether they are involved in the passage of ions through the pore.

Ion-Channel Activities of Cry4Ba-R158 Mutant Toxins

We have previously shown that when E. coli cells expressing each type of the Cry4Bahelix 4 mutant toxin were tested for their relative toxicity against A. aegypti larvae, four mutants with alanine substitutions at charged residues (Arg-143, Lys-156 and Glu-159) or at one polar residue (Asn-151) exhibited no loss of larvicidal activity. In contrast, one mutant with the alteration of a charged amino acid at Arg-158 was not active against the larvae. When this critical arginine residue at position 158 was converted to Gin, Glu or even to the most conserved residue for positively charged side chain, i.e. Lys, all R158 mutants (R158Q, R158E and R158K) were shown to be nontoxic to mosquito larvae (see Table 1). These results could imply the requirement for the specific structure of the positively charged side chain at this position. Perhaps Arg-158, which is likely to face the pore lumen, could interact with an aqueous environment and thus somehow stabilise the functional pore. However, the precise function of this residue remains to be elucidated. This notion is supported by experimental results obtained with directed substitutions of helix 4 residues in other Cry proteins, Cry1Aa, Cry1Ac Kumar & Aronson, 1999; Masson et al., 1999] and Cry11Aa (as shown previously). In order to test whether the loss of larvicidal activity in the Arg-158 mutants arises from the failure to form an active ion channel across lipid membranes of the larval midgut cells. A receptor-free, lipid membrane system i.e. planar lipid bilayers (PLBs) was employed to investigate ion channel properties of the mutant toxins in comparison with the wild type toxin. When the 65-kDa FPLC-purified Cry4Ba mutant toxins with substitutions at Arg-158 and/or Glu-159 were subjected to PLBs, all of the mutant toxins (R158A, R158K and E159A) were still able to form ion channels in the lipid membranes at the equivalent concentrations as that of the wild type toxin (150-300 nM). However, the activated R158A, R158K and E159A mutant toxins formed ion channels in the lipid bilayers with a decrease in maximum conductance values of ca. 200, 50 and 120, respectively (see Table 1).

Channel Properties of the Cry4Ba-α1-α5 Fragment

In symmetrical condition, PPF (α 1- α 5) channels were formed after a few minute (less than 30 min). Representative current steps of the PPF channels are illustrated in Fig. 4A & B. It was found in all experiments that the channels remained at an opened state. In some experiment, the main opening levels had changed (increase or decrease) when they were recorded for a period of time. When performed the experiment at 430 nM (or 10 μ g/mL) of the PPF proteins, the channels showed very high conductance values, which were higher than Cry4Ba channel. An attempt was performed to use low concentrations of protein (4.3 - 8.6 nM) and it was found that most of the conductances were lower than 1000 pS.

The channel formed by the PPF fragment also showed multiple conductance levels, i.e. main opening states, between 148 and 3243 pS. Thus the conductances were categorized into many levels. The criteria for sorting the conductances was the conductance that gave the standard error of means (SEM) more than 70 pS were sorted into different category. The I-V curves were also rectilinear that indicated the channel did not rectify (Fig. 4C). The channel formed by PPF fragment was remarked to have two different kinetics. Fast kinetic behavior was observed in three experiments at some applied voltages (Fig. 4B).

Ion selectivity was measured by conducting experiments under asymmetrical condition 450/150 mM KCl (cis/trans). The I-V curves showed reverse potential (VR) at -17 ± 1.0 mV. According to Nernst equation, the Nernst potential for K+ under this condition used was -17 mV demonstrating cationic selective channel. As calculated from VR using the GHK equation, the P_K / P_{Cl} permeability ratio was 4.5, indicating selectivity for K⁺ over Cl⁻. These results clearly showed that $\alpha 1-\alpha 5$ of the Cry4Ba toxin could exerted ion-channel activity efficiently without the remainder of the 65-kDa activated Cry4Ba toxin.

Simulations of Hexameric α4-α5 Pore Models of Cry4Ba and It Mutants

Simulated anneal/molecular dyanamics (SA/MD) of the Cry3Aa-α5 fragment suggested that this helical peptide was able to form a stable hexameric pore [Kerr et al., 1994]. Mean field Monte Carlo simulations showed that this conserved transmembrane helix also has high competency of inserting into a continuum hydrophobic slab [Biggin & Sansom, 1996]. Here, MD simulations were integrated with the previous experimental evidences to build a pore model

mediated by the Cry4Ba-transmembrane helical hairpin, α4-loop-α5, residues Q140-E198, (see Fig. 5).

The Cry4Ba-transmembrane α 4-loop- α 5 hairpin was successfully placed in an equilibrated system of 128-molecule palmitoyl-oleyl-phosphatidylcholine (POPC) bilayers. After the system was subjected to 100 psec of positional restrained MD simulations, unrestrained MD simulations of the system were carried for 2 nsec. Trajectories of atom coordinates were then examined for structural and energy changes. It was found that after 1 nsec of MD simulations, the RMS values of positional displacement and total energy of the system became fluctuating at a certain value indicating that the system has reached an equilibrium stage (data not shown). The snapshots of the protein/POPC bilayers showed a stable helical hairpin-liked structure of which the amphipathic α 4 helix was stabilised by favorable interactions between pockets of membrane-penetrating water molecules and side chains of polar residues while the relatively hydrophobic α 5 helix appeared to unwind at its C-terminus (data not shown).

Models of 3-10 subunits of the Cry4Ba α 4-loop- α 5 hairpin were initially constructed and their internal radii were determined via HOLE 2.0. The hexameric model of which pore radius corresponds to the experimentally estimated pore diameter for the Cry1Ac toxin [Knowles & Ellar, 1987] was chosen as a representative for a pore model of Cry4Ba with Arg-158 pointing inward to pore lumen. By using *in vacuo* SA/MD, 25 distinctive models were generated. Self RMSD values were calculated [Kerr et al., 1994] and the most symmetric pore model was subjected to MD simulations. Unrestrained MD simulations were performed with the pore model placed in an equilibrated POPC/water bilayer system within 2-nanosecond simulations. As can be seen from the ribbon representative in Fig. 6, the hexameric models reveal that both α 4 and α 5 remain their helical conformation, but the predicted α 4- α 5 loop develops a helical structure, suggesting that membrane insertion and oligomerisation could induce structural changes of the transmembrane fragments.

The equilibrated coordinates of the wild type Cry4Ba system were used as a template for simulations of the mutant systems. Different amino acids were substituted into the Cry4Ba pore model, generating pore models of R158A, R158K and E159A. The simulated pore models for both the Cry4Ba wild type and its mutant pore models were then subjected to MD simulations for another 1 nsec. Resulting trajectories (.XTC) and energy (.EDR) files from each simulated system were subjected to further analysis for trajectory and energy changes. The final coordinates of the simulated models for the three mutants show a helical arrangement similar to the wild type-pore model (data not shown). Analysis for the pore dimension showed that the radius near the constriction in the R158A model is ~1 Å larger than that in the wild type

and E159A models, indicating that the mutations at the critical Arg-158 residue could structurally affect the cavity of the pore models (see Fig. 7). Perhaps the lack of Arg-158 in α4 might destabilise the oligomeric structure of the Cry4Ba toxin-induced pore.

Specific Mutations within the α4-α5 Loop of Cry4Ba

As predicted from the homology-based 3D model of Cry4Ba, the α4-α5 loop comprises eight amino acids of which one is charged i.e. Glu-171 and two are polar i.e. Asn-166 and Tyr-170. With the exception of Asn-166, both Tyr-170 and Glu-171 are structurally conserved among the known Cry toxins (see Fig. 8A & B) that these loop residues could play a crucial role in Cry4Ba toxicity. In this study, we therefore initially generated three Cry4Ba loop mutants in which Asn-166, Tyr-170 and Glu-171 were substituted with alanine via PCR-based directed mutagenesis. When each mutant toxin was expressed in *E. coli* upon IPTG induction, they were all predominantly produced as sedimentable inclusion bodies and the protein expression level was comparable to the wild type Cry4Ba toxin. In addition, all the purified mutant inclusions were found to be soluble in carbonate buffer, pH 9.0, giving ca. 70% solubility which resembles closely to the wild type inclusions under similar conditions. The 130-kDa solubilised mutant protoxins were also assessed for their proteolytic stability by digestion with trypsin and all found to produce two major trypsin-resistant products of ca. 47 kDa and 18 kDa, identical to the wild type. These results suggested that each point mutation of these loop residues had no apparent effect on proteolytic processing and protein folding.

To determine an effect of the loop mutations on toxicity, *E. coli* cells expressing each type of the mutant toxin were tested for their relative biological activity against 2-day old A. aegypti larvae. All bioassays were carried out in ten replicas for each sample and repeated at least three times, the mortality data recorded after a 24-h incubation are shown in Fig. 9. Alanine substitutions of Asn-166 and Tyr-170 almost completely abolished the Cry4B bioactivity, although mutation at Glu-171 showed only a small decrease in larvicidal activity. These results suggested that Asn-166 and Tyr-170 play an important role in larvicidal activity of the Cry4Ba toxin.

When Asn-166 was further substituted with Asp, Gln, Arg, Cys or Ile, it revealed that substitutions of Asn-166 with polar amino acids could retain over 80% of the wild type toxicity while substitution with a non-polar residue *i.e.* isoleucine almost totally abolished the toxicity (see Fig. 9). All the Asn-166 mutant toxins were tested for toxin stability and revealed that they all produced stable, trypsin-resistant products. These results suggested that the polarity at position 166 located in the α4-α5 loop is important for larvicidal activity of the Cry4Ba toxin.

From molecular modelling of a putative toxin-induced pore consisting of six copies of the α4-α5 helical hairpin of Cry4Ba (see Fig. 10A), Asn-166 points toward the pore lumen and could form hydrogen bonds with water molecules. A crucial role in toxin mechanism at this critical position is conceivably to be involved in the formation of hydrogen bonds with water to stabilise the loop structure or it may be involved in the passage of ions through the channel (Fig. 10A). Whether these possibilities can be generalised remains to be elucidated.

For Tyr-170, it was also converted to Asp, Arg, Leu, Trp or Phe. Interestingly, substitutions of this critical tyrosine residue with only the aromatic residues (Trp or Phe) were shown to remain Cry4Ba toxicity against mosquito larvae (Fig. 9). Also, their protein expression levels, inclusion solubility and proteolytic stability suggested that the drastic loss of toxicity observed for the three other inactive mutants (Y170D, Y170R and Y170L) is unlikely to be caused by misfolding of the protein. These results together with the fact that the tyrosine residue at this position is a highly conserved amino acid among the Cry toxins strongly imply a general requirement for an aromatic structure at this crucial position. In several membrane proteins, a variety of roles have been proposed for the aromatic residues, especially Tyr and Trp in the transmembrane helices, which are preponderantly found at or near the membranewater interface. These roles include facilitating translocation of the periplasmic portion of proteins through the membrane, acting as determinants of protein orientation, introducing rigidity to the periphery of the transmembrane segments, or allowing vertical mobility of the transmembrane helical region with respect to the membranes. Considering all of the above, a function for Tyr-170 within the α4-α5 loop of Cry4Ba may conceivably be an interaction with the phospholipid head groups for stabilising the oligomeric pore structure (Fig. 10B).

Directed Mutations within the α4-α5 Loop of Cry4Aa

Based on multiple sequence alignments of the known Bt Cry toxin structures and the homology-based Cry4 models, the interhelical loop connecting $\alpha 4$ and $\alpha 5$ of the Cry4Aa toxin is composed of sixteen amino acids with the majority being polar and charged residues (Fig. 8A). Previously, we have shown that polarity and aromaticity for Asn-166 and Tyr-170, respectively, in the $\alpha 4$ - $\alpha 5$ loop are critically involved in tarvicidal activity of the Cry4Ba toxin (see above). Here, we have also constructed several mutants in the $\alpha 4$ - $\alpha 5$ loop region of Cry4Aa in order to determine a residue responsible for the toxin activity. Two negatively charged (Asp-198 and Asp-200) and four polar (Asn-190, Asn-195, Tyr-201 and Tyr-202) residues were selected for initially substitution with alanine via PCR-based directed

mutagenesis. The loop mutant toxins were expressed in *E. coli* under inducible control of the *tac* promoter. Upon addition of IPTG to the mid-exponential phase cultures, all mutant Cry4Aa protoxins were predominantly produced in the form of sedimentable inclusion bodies. When *E. coli* lysates were analysed by SDS-PAGE, the levels of protein expression for all mutants were found to be comparable to that of the wild-type (data not shown).

To assess the solubility of the mutant protoxin inclusions in comparison with that of the wild-type, experiments were carried out using carbonate buffer, pH 10.0. The amounts of the 130-kDa Cry4Aa soluble proteins in the supernatant were compared with those of the proteins initially used so as to determine the percentage of toxin solubilisation. The toxin inclusions of the N190A, D198A, D200A and Y201A mutants were soluble in this buffer, giving approximately 60-70% solubility, which is comparable to the solubility of the wild-type inclusions under similar conditions. On the other hand, a nearly complete loss of the inclusion solubility was observed for the two remaining mutants, N195A and Y202A (see Fig. 11). However, toxin inclusions of the two closely related loop-Cry4Ba mutants, N166A and Y170A as mentioned earlier, were found to be relatively soluble in this buffer (see above). At this stage, the reason for this difference in solubility between the two loop-mutants of Cry4Aa and Cry4Ba is unclear. It does however lead to the interesting possibility that single-alanine substitutions at Asn-195 and Tyr-202 of the Cry4Aa toxin could disturb the structural characteristics that consequently affect toxin-inclusion formation as shown by a drastic decrease in solubility.

To determine the effect of the α4-α5 loop mutations on the Cry4Aa bioactivity, *E. coli* cells expressing each mutant toxin were tested for their biological activity towards *A. aegypti* mosquito-larvae. Replacement at only Tyr-202 with alanine almost completely abolished larvicidal activity, whereas alanine-substitutions at the other positions (Asn-190, Asn-195, Asp-198, Asp-200 and Tyr-201) did not affect the Cry4Aa toxicity. Further analysis *via* specific mutations revealed that conversion of this critical tyrosine residue to cysteine resulted in a drastic loss of toxicity, whilst replacement with the aromatic residue *i.e.* phenylalanine, still retained the high level of larvicidal activity (see Fig. 12). The level of protein expression of both Y202C and Y202F mutant toxins was approximately the same as that of the wild-type. These results, together with the highly structural conserved level of the tyrosine residue at this position among the Cry toxins (see Fig. 8B), suggest an essential feature of an aromatic structure at this critical position for the toxin activity. The data further support our previous findings that Tyr-170 in the α4-α5 loop plays an important role in larvicidal activity of the 130-kDa Cry4Ba toxin, since substitutions with only the aromatic residues, *i.e.* Phe or Trp, were shown to restore the bioactivity towards mosquito-larvae (see above).

April 10 Hard Title \$1000 Inch.

For *in vitro* solubility, like the Y202A mutation, the substitution of Tyr-202 with Cys reduced the solubility *in vitro* of toxin inclusions, while a conversion to Phe still exhibited the same solubility characteristics as that of the wild-type (data not shown). Although insolubility of toxin inclusions and the loss of toxicity are seemingly correlated for both Y202A and Y202C mutants, the inclusion solubility *in vitro* may not necessarily reflect toxin activity *in vivo* as observed for the N195A mutant which was insoluble in the carbonate buffer, but still bioactive (see Fig. 12). It has been demonstrated that single-proline substitution in α6 of Cry4Ba dramatically perturbed the inclusion dissolvability, but did not affect its larvicidal activity [Sramala *et al.*, 2000]. Also, it has been shown that the difference detected in solubilisation *in vitro* for the cloned Cry4Aa toxin inclusions, which were purified form two different *Bt* recipient strains, is not a factor for toxicity *in vivo* [Angsuthanasonbat *et al.*, 1992]. Presumably, the larval gut proteases *in vivo* might facilitate the dissolution of the ingested toxin inclusions that would negate the differences between the observed larvicidal activities of the bioactive N195A and non-active Y202A or Y200C mutants.

Studies with several membrane proteins have indicated that the aromatic residues are predominantly found at or near the lipid-water interface [Ulmschneider & Sansom, 2001]. These aromatic residues have been proposed to function in anchoring the proteins into the membrane through interactions of their aromatic rings with phospholipid head groups [Yau et al., 1998; Killian & Von Heijne, 2000], maintaining rigidity in the periphery of the transmembrane segments [Tsang & Saier, 1996], allowing vertical mobility of the transmembrane helical region with respect to the membranes, facilitating translocation of the periplasmic portion of proteins through the membrane, thereby acting as determinants of protein orientation [Schiffer et al., 1992]. Taken together, a function for Tyr-202 in the α4-α5 loop of the Cry4Aa toxin may conceivably be an interaction with the phospholipid head groups for stabilising the oligomeric pore structure.

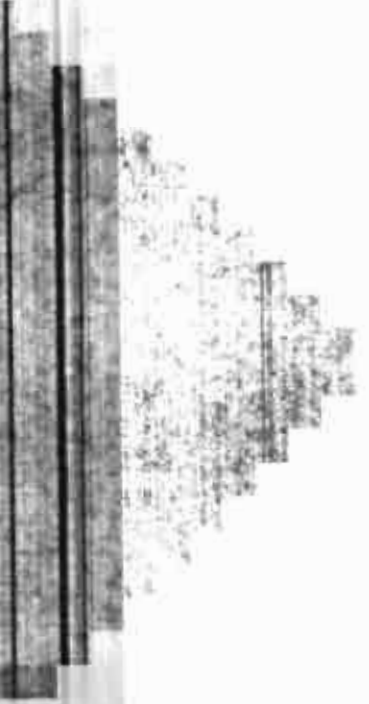
In conclusion, this study additionally demonstrates that the aromaticity of Tyr-202 in the α 4- α 5 loop plays a crucial role in the Cry4Aa toxicity that further supports the notion that the aromatic structure of the highly conserved tyrosine residue within the loop connecting the two transmembrane helices, α 4 and α 5, is essential for toxic action of the Bt Cry δ -endotoxins. However, further studies are still required to elucidate the exact role of this critical residue in toxin function.



Table 1 Effects of point mutations at charged amino acid residues in α4 of Cry4Ba

Sample	α4 sequence	Mortality* (%)	Conductance b (pS)
Wild type	Q140SYRTAVITQFNLTSAKLRETAVYFS165	92.0 ± 1.0	536
R158A	Q ₁₄₀ S ₁₆₅	0.0	210
R158K	Q ₁₄₀ S ₁₆₅	1.0 ± 0.6	51
R158Q	Q ₁₄₀ S ₁₆₅	1.3 ± 0.7	*
R158E	Q ₁₄₀ S ₁₆₅	1.0 ± 0.0	
E159A	Q ₁₄₀ S ₁₆₅	89.3 ± 2.9	120

Mortality of A. aegypti larvae recorded after 24-hour incubation with partially purified protoxin inclusions (5 mg/mL). The data represent the mean ± SEM based on 4 or 5 independent experiments.



The data represent the mean ± SEM of conductance values at maximum opening state based on 3-5 independent experiments.

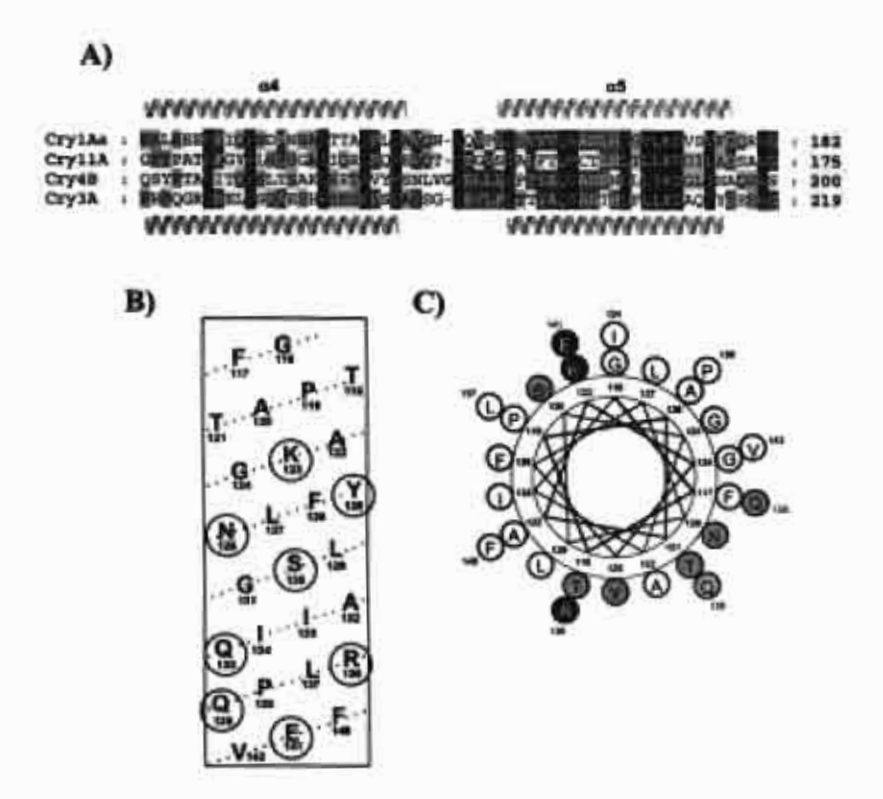


Figure 1 (A): Multiple sequence alignment of helices 4 and 5 of Cry11Aa with the crystal structures of Cry1Aa and Cry3Aa and the homology-based model of Cry4Ba. The sequences were aligned using the program CLUSTAL W. The degree of conservation is represented by background shading of the residues, with the darkest shading for the most conserved: 100% conserved, 75% conserved and 50% conserved. The positions of secondary structure elements of Cry1Aa and Cry3Aa are illustrated over and under the alignments, respectively. (B): The predicted pattern of helix 4 of Cry11Aa is composed of 27 residues of which the encircled residues were mutated. (C): A helical wheel projection of helix 4 of Cry11Aa. Amino acid residues are plotted every 100 degrees consecutive around the wheel, following the sequences given in B. The following colour code is used: black is an amino acid with a charged side chain; gray is a polar side chain and white is a hydrophobic side chain.

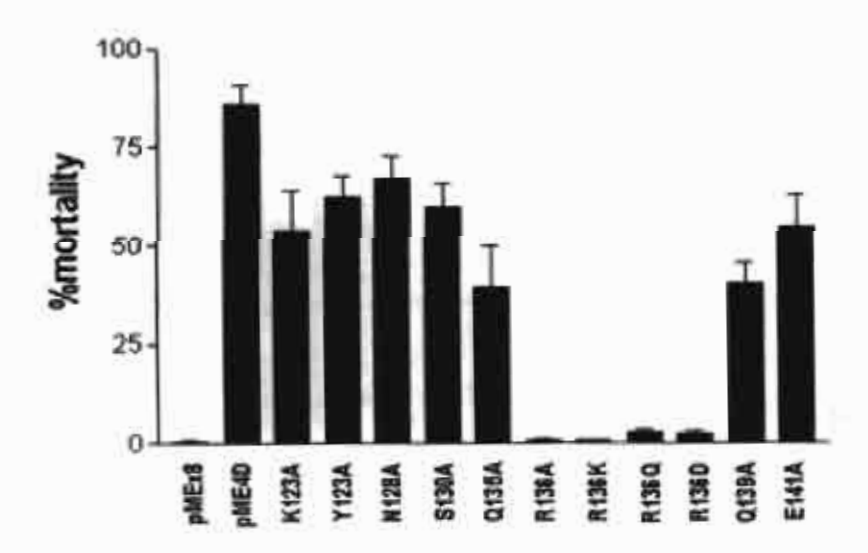


Figure 2 Mosquito-larvicidal activities of *E. coli* cells expressing the Cry11Aa wild-type toxin (pME4D) or its mutants (K123A, Y125A, N128A, S130A, Q135A, R136A, R136K, R136Q, R136D, Q139A and E141A) against *A. aegypti* larvae. Error bars indicate standard error of the mean from three independent experiments.

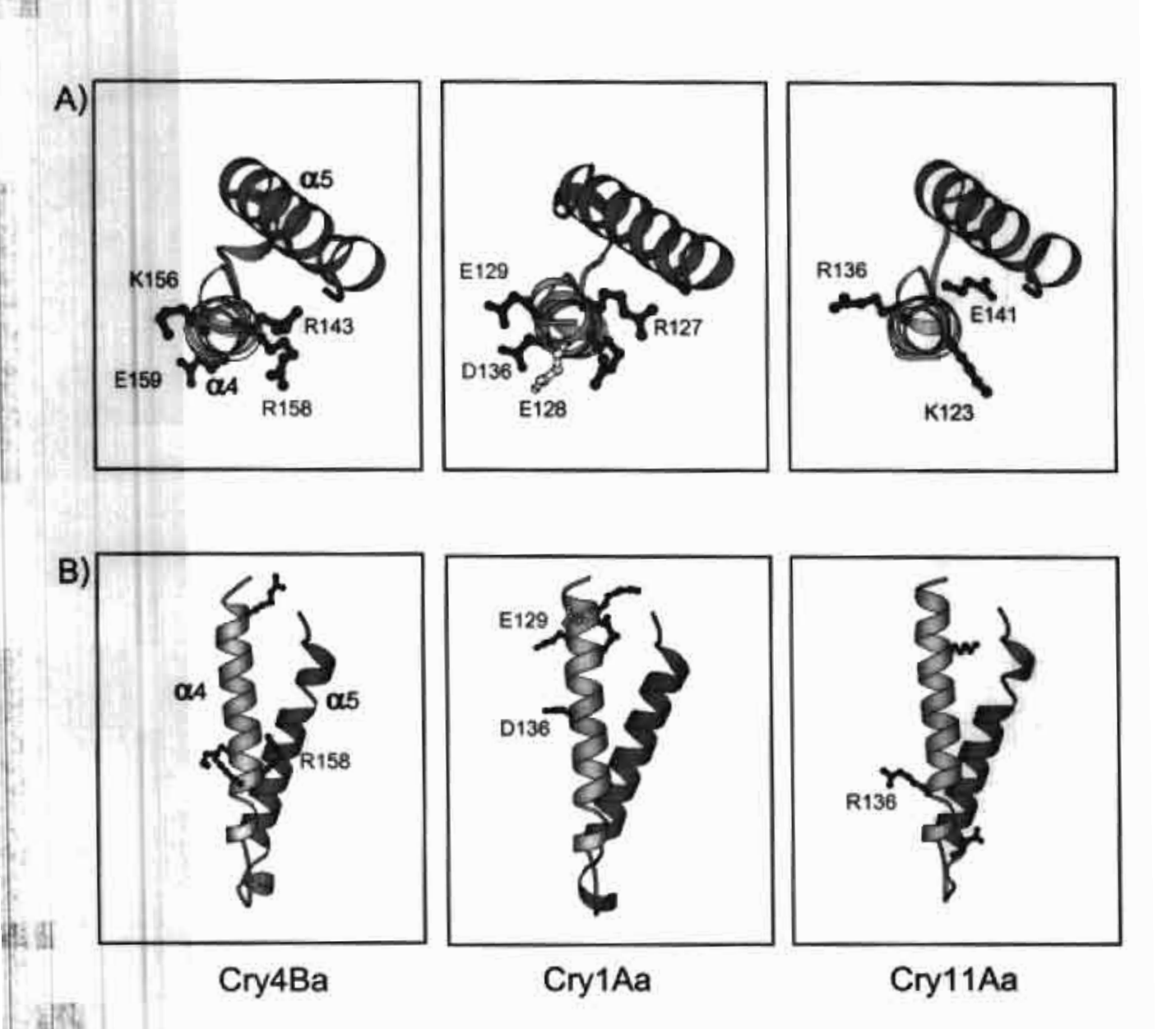


Figure 3 Top (A) and side (B) views of the α4-α5 hairpin of Cry4Ba, Cry1Aa, and Cry11Aa are illustrated in ribbon representations. α4, α5 and loop region are shown. Charged residues are shown with balls and sticks. Residues shown in bold indicate the biologically critical charged residues. Grey residues indicate non-critical charged residue. There is no mutation study report for the residue shown in white.

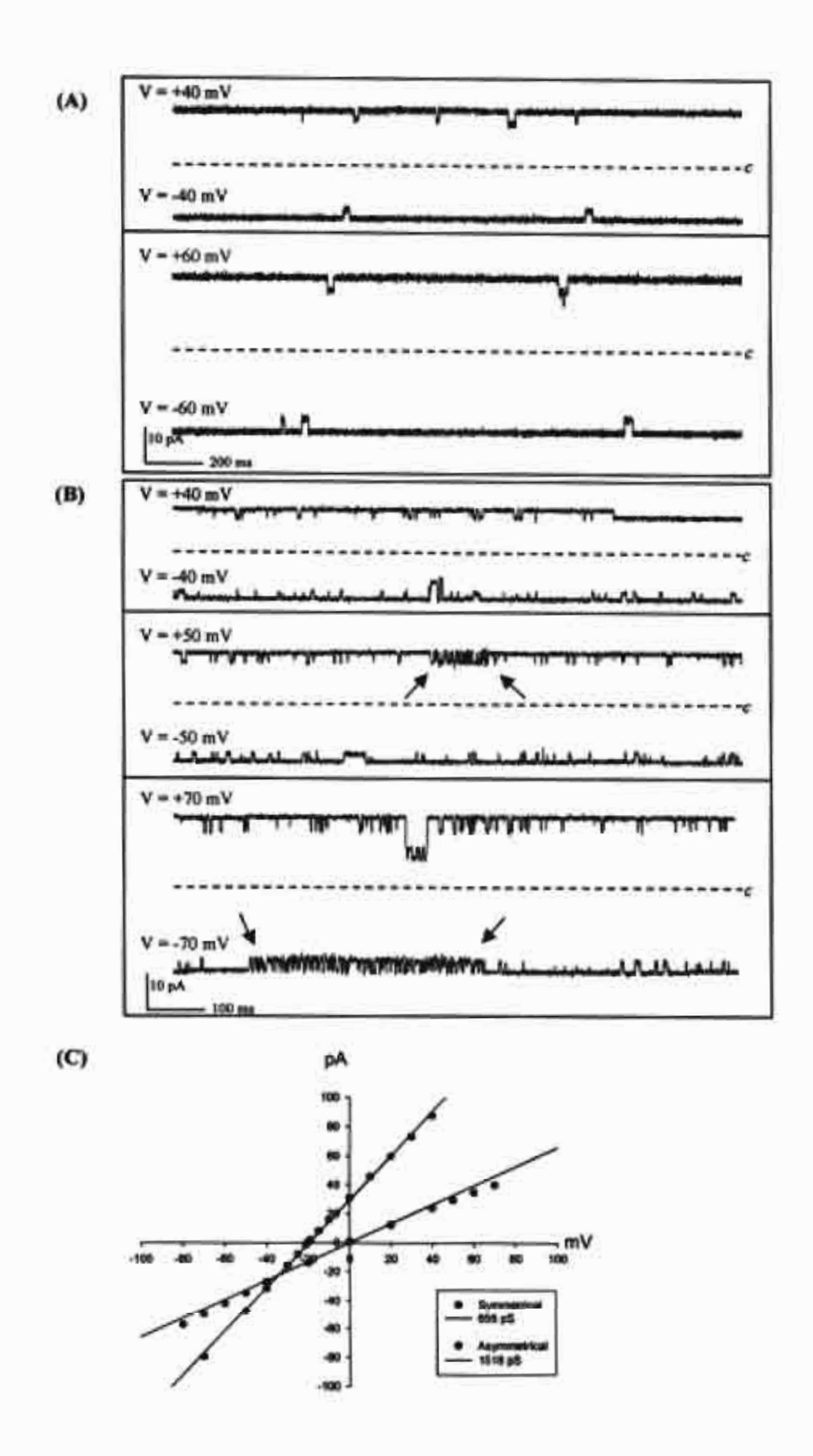


Figure 4 Channel current traces of PPF channels observed in symmetrical condition 150mM KCl solution.

(A) and (B): Representative records at various holding voltages (V) indicated next to the traces. The letter c indicates the closed state of the channels. (A) and (B) represent the low and high activities of PPF channels. Fast kinetic was pointed with the black arrows. (C) Current-voltage relations obtained from currents recorded in symmetrical and asymmetrical conditions. Data points were fitted by linear regression. The conductance of each trace is shown directly in the box. The reversal potential is shifted to −19 mV demonstrating cationic channel selectivity.

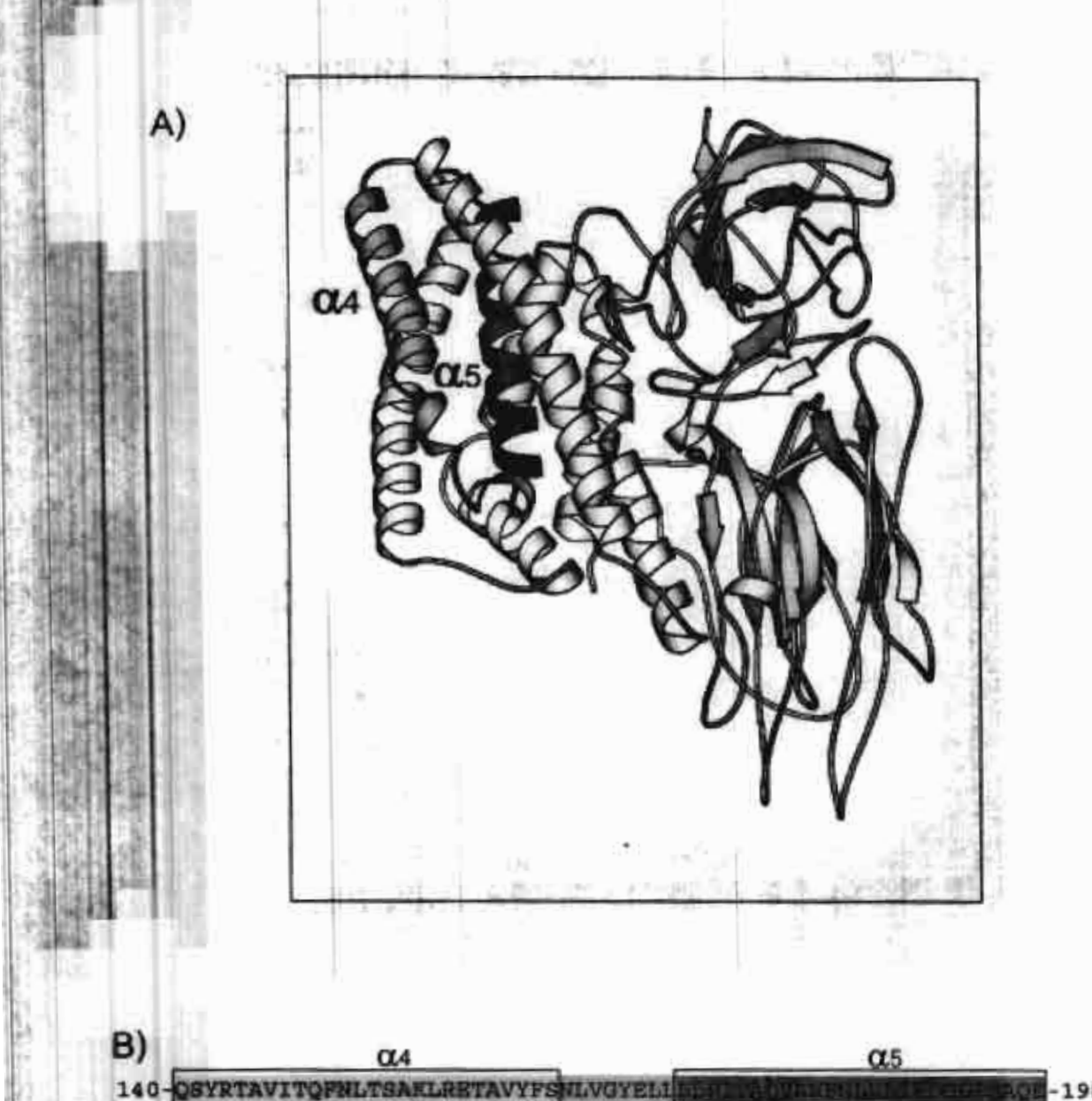


Figure 5 (A) 3D model for Cry48a constructed by homology modeling. Shaded helices represent α4 and α5, respectively. Loop between α4 and α5 is shown in gray. (B) Amino acid sequence of the transmembrane fragment α4-loop-α5 hairpin which is shown in single-letter code. The helical regions are indicated with rectangular boxes.

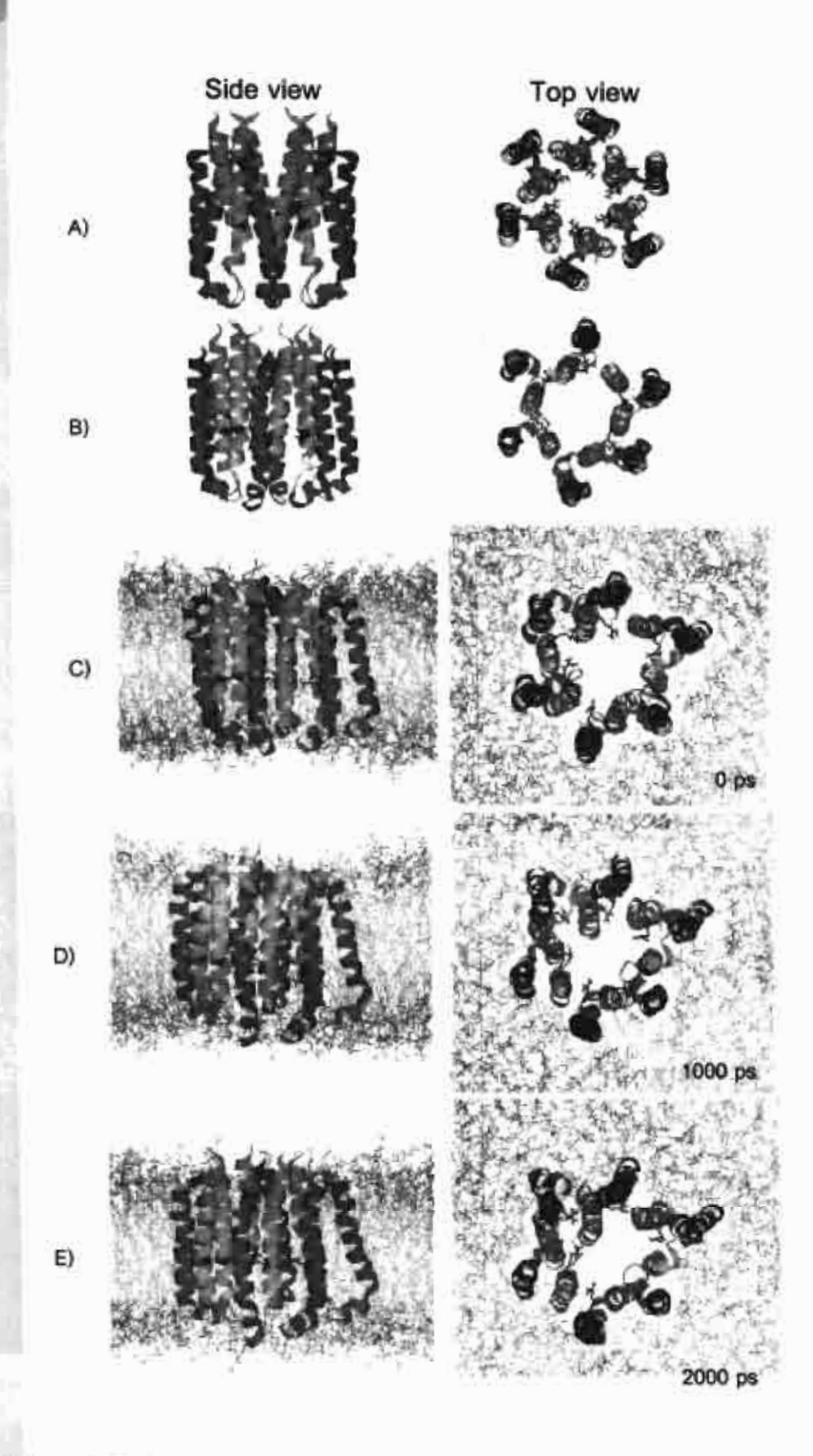


Figure 6 Top and side views of hexameric pore models for Cry4Ba comprising 6 copies of the Cry4Ba α4α5 hairpin in POPC bilayers before (A) and after (B) SA / MD which shows α4, α5 and the α4-α5. Arg-158 residues are drawn explicitly in gray stick. Snapshots of the pore in POPC/water bilayers at 0, 1000 and 2000 psec (C-E) are shown in ribbon representatives. POPC molecules are shown in sticks. Water molecules are omitted for clarity.

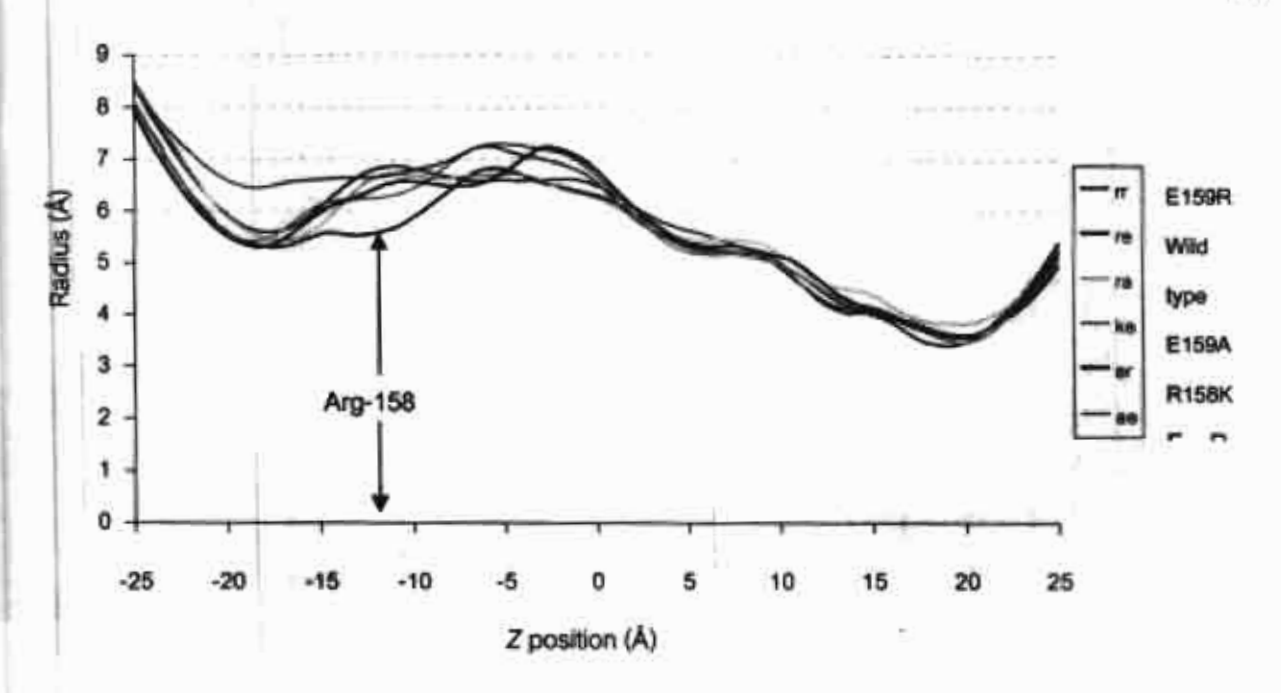


Figure 7 The figure shows effective radii along Z axis of the simulated Cry4Ba hexameric pore models. The profile pore radius of each model is averaged from 1000 psec simulations. Arrows indicate the approximated position of Arg-158.

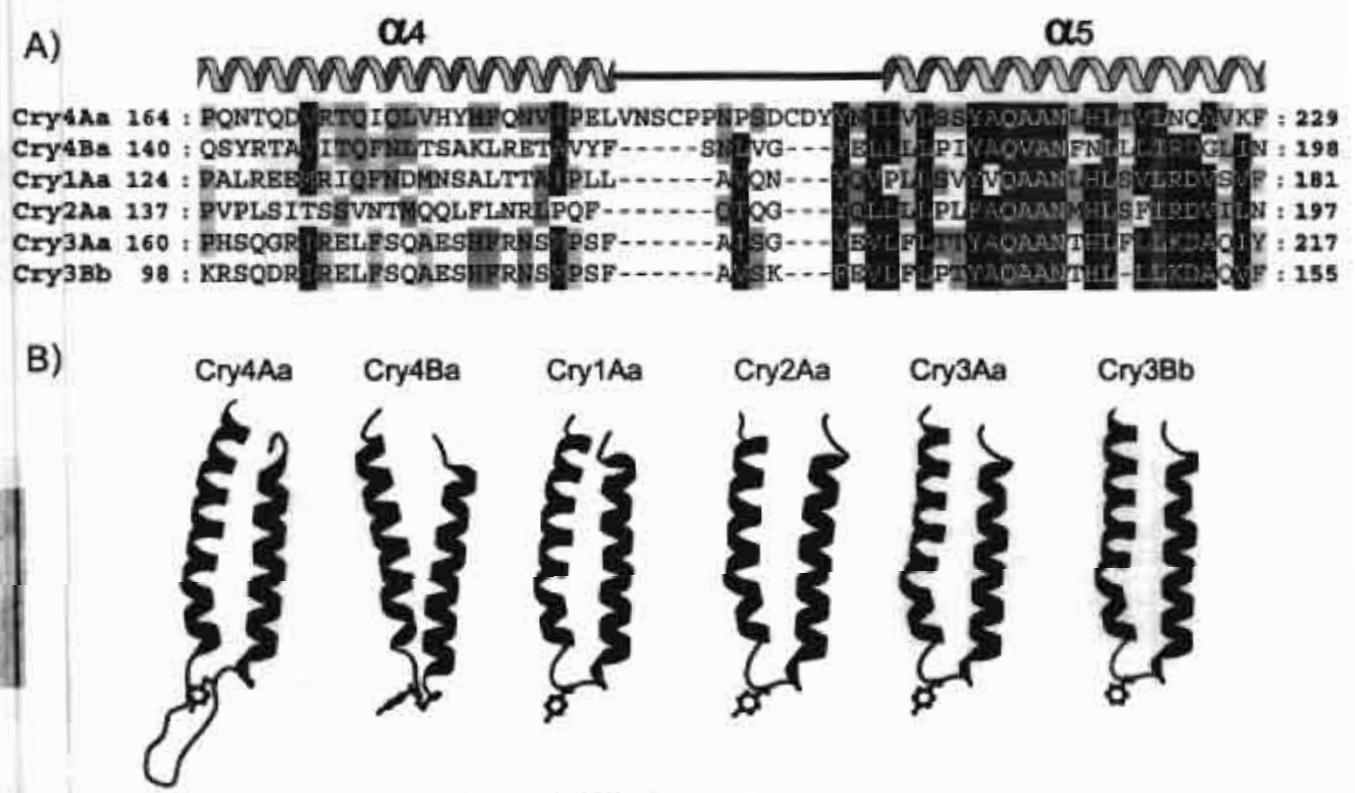


Figure 8 (A) Multiple sequence alignment of the transmenbrane α4-loop-α5 fragment of Cry4Aa with those of the crystal structures of Cry1Aa, Cry2Aa, Cry3Aa and Cry3Bb toxins and the homology-based Cry4Ba model. The sequences were aligned using the program Clustal X. The corresponding α4-loop-α5 is shown above the sequences. (B) Side views of the α4-loop-α5 helical hairpins of the homology-based Cry4Aa and Cry4Ba models, and the known structures of Cry1Aa, Cry2Aa, Cry3Aa and Cry3Bb. Gray ribbons represent α4 and α5. The conserved loop-residue, Tyr, is shown in ball-and-stick in all six helical hairpins.

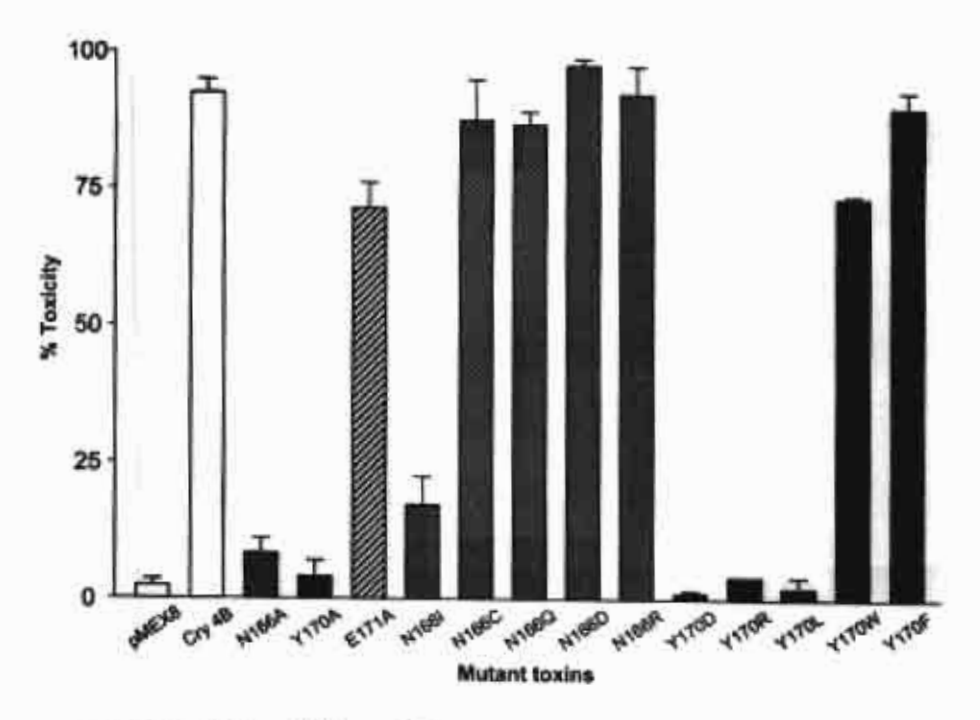


Figure 9 Mosquito-larvicidal activities of *E. coli* cells expressing the wild type toxin or mutant toxins (N166A, Y170A, E171A, N166I, N166C, N166Q, N166D, N166R, Y170D, Y170R, Y170L, Y170W and Y170F) against *A. aegypti* larvae. Error bars indicate standard error of the means from three independent experiments.

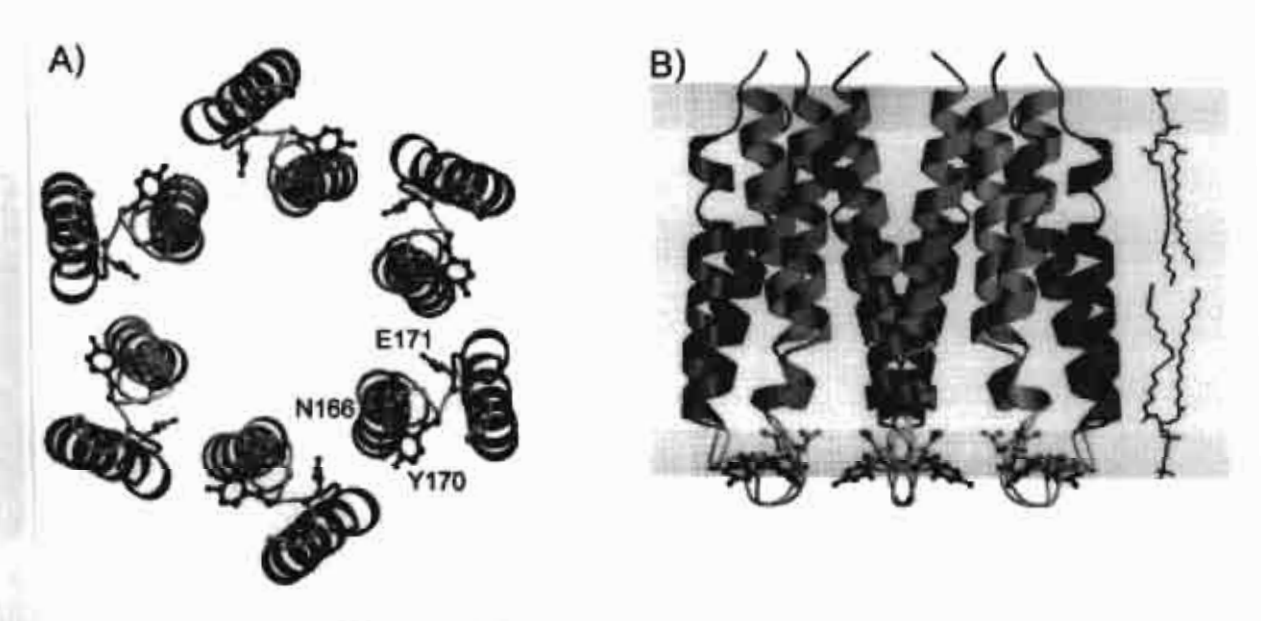


Figure 10 (A) Bottom view of the model of a putative oligomeric pore consisting of six copies of the α4-α5 hairpin of the Cry4Ba toxin. Asn-166, Tyr-170 and Glu-171 are shown. (B) The Tyr-170 residues are found at the membrane-water interface after oligomerization and pore formation. Rectangular boxes represent the planar lipid membrane bilayers. Helices 4 and 5 are shown as gray strands.

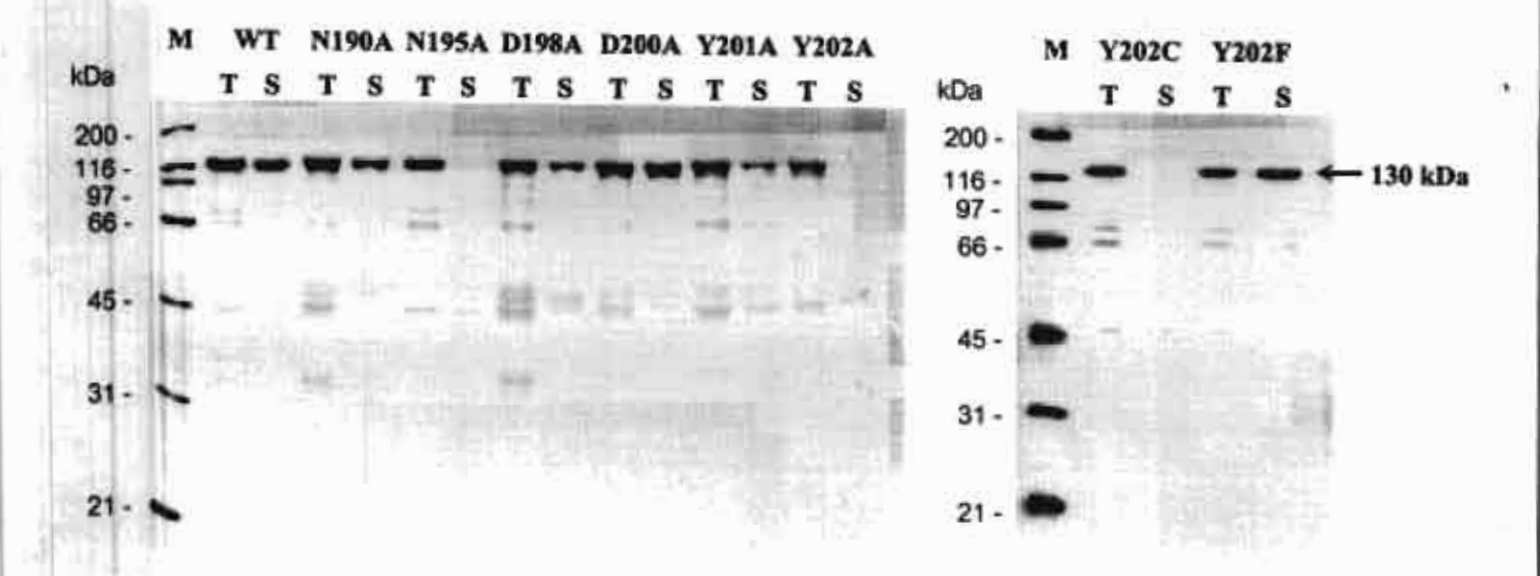


Figure 11 SDS-PAGE (Coomassie brilliant blue-stained 10% gel) analysis of the partially purified 130-kDa protein inclusions extracted from *E. coli* expressing the wild-type (WT) and Cry4Aa mutant toxins and solubilised in carbonate buffer, pH 10.0. (T) and (S) represent total fractions and an equivalent volume of the supermatants after centrifugation, respectively. (M) represents the molecular mass standards.

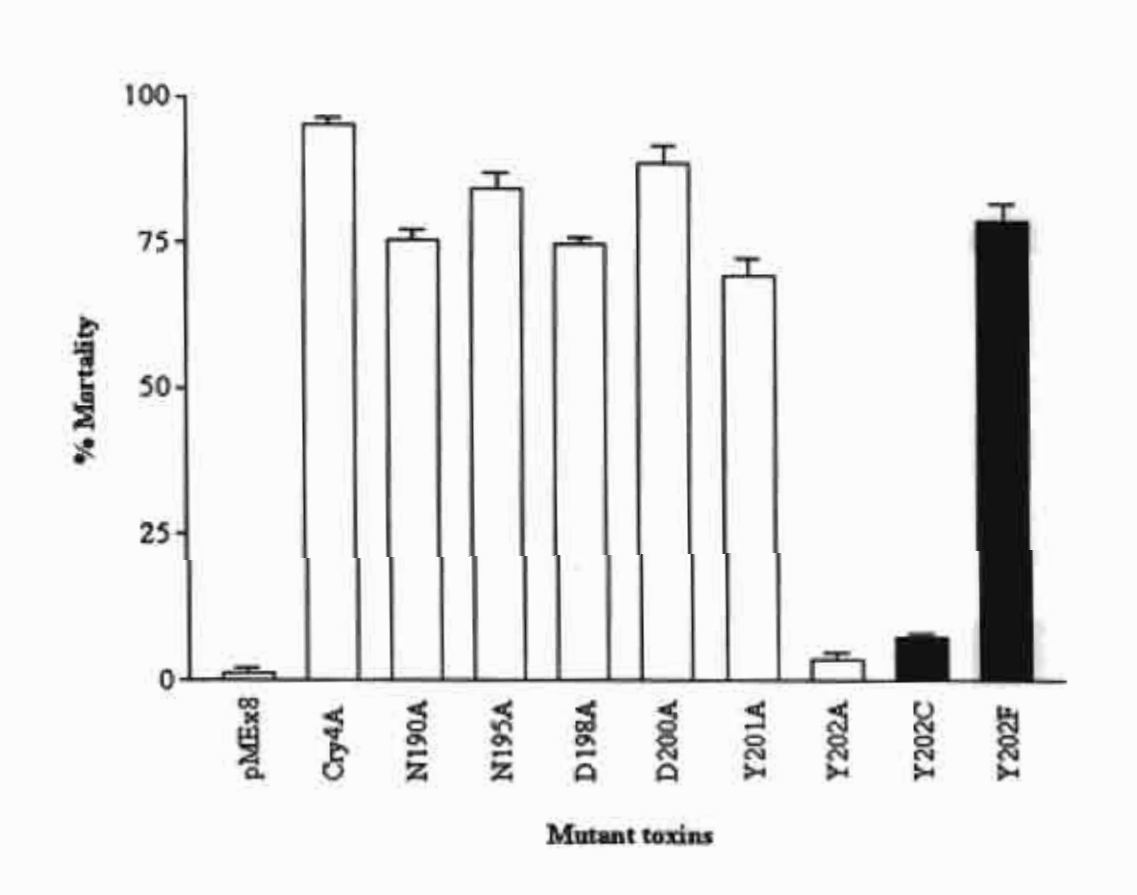


Figure 12 Mosquito-larvicidal activities of E. coll cells expressing the Cry4Aa wild-type or its mutant toxins (N190A, N195A, D198A, D200A, Y201A, Y202A, Y202C and Y202F) against A. segypt/ larvae. Error bars indicate standard errors of the mean from three independent experiments.

References

- Angsuthanasombat, C., Chungjatupornchai, W., Kertbundit, S., Luxananil, P., Settasatian, C., Wilairat, P. and Panyim, S. (1987) Cloning and expression of 130-kd mosquito-larvicidal delta-endotoxin gene of *Bacillus thuringiensis* var. israelensis in Escherichia coli. Mol. Gen. Genet. 208, 384-389.
- Angsuthanasombat, C., Crickmore, N. and Ellar, D.J. (1991) Cytotoxicity of a cloned Bacillus thuringiensis subsp. israelensis CryIVB toxin to an Aedes aegypti cell line. FEMS Microbiol. Lett. 83, 273-276.
- Angsuthanasombat, C., Crickmore, N. and Ellar D.J. (1992) Comparison of Bacillus thuringiensis subsp. israelensis CrylVA and CrylVB cloned toxins reveals synergism in vivo. FEMS Microbiol. Lett. 94, 63-68.
- Angsuthanasombat, C., Crickmore, N. and Ellar, D.J. (1993) Effects on toxicity of eliminating a cleavage site in a predicted interhelical loop in the *Bacillus thuringiensis* CryIVB δ-endotoxins. FEMS Microbiol. Lett. 111, 255-262.
- Aronson, A.I., Beckman, W. and Dunn, P. (1986) Bacillus thuringiensis and related insect pathogens. Microbiol. Rev. 50, 1-24.
- Biggin, P.C. and Sansom, M.S. (1996) Simulation of voltage-dependent interactions of alpha-helical peptides with lipid bilayers. *Biophys. Chem.* 11, 99-110.
- Buttcher, V., Ruhlmann, A. and Cramer, F. (1990) Improved single-stranded DNA producing expression vectors for protein manipulation in *Escherichia coli. Nucleic Acids Res.* 18, 1075.
- Fox, J.A. (1987) Ion channel subconductance states. J. Membr. Biol. 97,1-8.
- Crickmore, N., Zeigler, D.R., Feitelson, I., Schnepf, E., Van Rie, J., Lereclus, D., Baum, J. and Dean, D.H. (1998) Revision of the nomenclature for the *Bacillus thuringiensis* pesticidal crystal proteins. *Microbiol. Mol. Biol. Rev.* 62, 807-813.
- Cummings, C.E., Armstrong, G., Hodgman, T.C. and Ellar, D.J. (1994) Structural and functional studies of a synthetic peptide mimicking a proposed membrane inserting region of a *Bacillus* thuringiensis delta-endotoxin. *Mol. Membr. Biol.* 11, 87-92.
- Galitsky, N., Cody, V., Wojtczak, A., Ghosh, D., Luft, J. R., Pangborn, W. and English, L. (2001).
 Structure of the insecticidal bacterial delta-endotoxin Cry3Bb1 of Bacillus thuringiensis. Acta
 Crystallogr. D. Biol. Crystallogr. 57, 1101-1109.
- Gazit, E., La Rocca, P., Sansom, M.S.P. and Shai, Y. (1998) The structure and organization within the membrane of the helices composing the pore-forming domain of *Bacillus thuringiensis* deltaendotoxin are consistent with an "umbrella-like" structure of the pore. *Proc. Natl. Acad. Sci.* USA 95, 12289-12294.

- Gerber, D. and Shai, Y. (2000) Insertion and organization within membranes of the delta-endotoxin pore-forming domain, helix 4-loop-helix 5, and inhibition of its activity by a mutant helix 4 peptide. J. Biol. Chem. 275, 23602-23607.
- Grochulski, P., Masson, L., Borisova, S., Pusztai-Carey, M., Schwartz, J.L., Brousseau R. and Cygler, M. (1995) Bacillus thuringiensis CrylA(a) insecticidal toxin: crystal structure and channel formation. J. Mol. Biol. 254, 447-464.
- Hill, B. (1992) Selective permeability: independence. In: Ionic Channels of Excitable Membranes; 2nd ed. Sinauer Associates, Sunderland, MA, USA, pp. 337-361.
- Hofte, H. and Whiteley H.R. (1989) Insecticidal crystal proteins of Bacillus thuringiensis. Microbiol. Rev. 53, 242-255.
- Kerr, I.D., Sankararamakrishnan, R., Smart, O.S. and Sansom, M.S. (1994) Parallel helix bundles and ion channels: molecular modeling via simulated annealing and restrained molecular dynamics. *Biophys. J.* 67,1501-1515.
- Killian, J.A. and Von Heijne, G. (2000) How proteins adapt to membrane-water interface. Trends Biochem. Sci. 25, 429-434.
- Knowles, B.H. (1994) Mechanism of action of Bacillus thuringiensis insecticidal δ-endotoxins. Adv. Insect Physiol. 24, 275-308.
- Knowles, B.H. and Ellar, D.J. (1987) Colloid-osmotic lysis is a general feature of the mechanism of action of Bacillus thuringiensis δ-endotoxins with different insect specificity. Biochem. Biophys. Acta. 924, 509-518.
- Kumar, A.S. and Aronson, A.I. (1999) Analysis of mutations in the pore-forming region essential for insecticidal activity of a *Bacillus thuringiensis* delta-endotoxin. *J. Bacteriol.* 181, 6103-6107.
- Li, J., Carroll, J. and Ellar, D.J. (1991) Crystal structure of insecticidal delta-endotoxin from Bacillus thuringiensis at 2.5 Å resolution. Nature 353, 815-821.
- Masson, L., Tabashnik, B.E., Liu, Y.B., Brousseau, R. and Schwartz, J.L. (1999) Helix 4 of the Bacillus thuringiensis Cry1Aa toxin lines the lumen of the ion channel. J. Biol. Chem. 274, 31996-32000.
- Morse, R.J., Yamamoto, T. and Stroud, R.M. (2001). Structure of Cry2Aa suggests an unexpected receptor binding epitope. Structure (Camb.). 9, 409-417.
- Nicholls, C.N., Ahmad, W. and Ellar, D.J. (1989) Evidence for two different types of insecticidal P2 toxins with dual specificity in *Bacillus thuringiensis* subspecies. *J. Bacteriol.* 171, 5141-5147.
- Nunez-Valdez, M.-E., Sanchez, J., Lina, L., Guereca, L. and Bravo, A. (2001) Stuctural and functional studies of α-helix 5 region from *Bacillus thuringiensis* Cry1Ab δ-endotoxins. *Biochimi. Biophys.* Acta. 1546, 122-133.
- Pawagi, A.B. and Deber, C.M. (1990) Ligand-dependent quenching of tryptophan fluorescence in human erythrocyte hexose transport protein. *Biochemistry* 29, 950-955.

- Schiffer, M., Chang, C.H. and Stevens, F.J. (1992) The functions of tryptophan residues in membrane proteins. Protein Eng. 5, 213-214.
- Schnepf, E., Crickmore, N., Van Rie, J., Lereclus, D., Baum, J., Feitelson, J., Zeigler, D.R. and Dean, D.H. (1998) Bacillus thuringiensis and its pesticidal crystal proteins. Microbiol. Mol. Biol. Rev. 62, 775-806.
- Schwartz, J.L., Garneau, L., Savaria, D., Masson, L., Brousseau, R. and Rousseau, E. (1993) Lepidopteran-specific crystal toxins from *Bacillus thuringiensis* form cation- and anion-selective channels in planar lipid bilayers. *J. Membr. Biol.* 132, 53-62.
- Schwartz, J.L., Juteau, M., Grochulski, P., Cygler, M., Prefontaine, G., Brousseau, R. and Masson, L. (1997) Restriction of intramolecular movements within the Cry1Aa toxin molecule of *Bacillus thuringiensis* through disulfide bond engineering. *FEBS Lett.* 410, 397-402.
- Sramala, I., Leetachewa, S., Krittanai, C., Katzenmeier, G., Panyim, S. and Angsuthanasombat, C. (2001) Charged residues screening in helix 4 of the *Bacillus thuringiensis* Cry4B toxin reveals one critical residue for larvicidal activity. *J. Biochem. Mol. Biol. Biophys.* 5, 219-225.
- Sramala, I., Uawithya, P., Chanama, U., Leetachewa, S., Krittanai, C., Katzenmeier, G., Panyim, S. and Angsuthanasombat, C. (2000) Single proline substitutions of selected helices of the Bacillus thuringiensis Cry4B toxin affect inclusion solubility and larvicidal activity. J. Biochem. Mol. Biol. Biophys. 4, 187-193.
- Tsang, S. and Saier, M.H., Jr. (1996) A simple flexible program for the computational analysis of amino acyl residue distribution in proteins: application to the distribution of aromatic versus aliphatic hydrophobic amino acids in transmembrane alpha-helical spanners of integral membrane transport proteins. J. Comput. Biol. 3, 185-190.
- Uawithya, P., Tuntitippawan, T., Katzenmeier, G., Panyim, S. and Angsuthanasombat, C. (1998)
 Effects on larvicidal activity of single proline substitutions in alpha 3 or alpha 4 of the Bacillus thuringiensis Cry4B toxin. Biochem. Mol. Biol. Int. 44, 825-832.
- Ulmschneider, M.B. and Sansom, M.S.P. (2001) Amino acid distributions in integral membrane protein structures. *Biochimi. Biophys. Acta* 1512, 1-14.
- Von Tersch, M.A., Slatin, S.L., Kulesza, C.A. and English, L.H. (1994) Membrane-permeabilizing activities of *Bacillus thuringiensis* coleopteran-active toxin CrylliB2 and CrylliB2 domain 1 peptide. *Appl. Environ. Microbiol.* 60, 3711-3717.
- Walters, F.S., Slatin, S.L., Kulesza, C.A. and English, L.H. (1993) Ion channel activity of N-terminal fragments from CrylA(c) delta-endotoxin. *Biochem. Biophys. Res. Commun.* 196, 921-926.
- Yau, W. M., Wimley, W. C., Gawrisch, K. and White, S. H. (1998) The preference of tryptophan for membrane interfaces. *Biochemistry* 37, 14713-14718.

Outputs

1. Publications

- 1.1 Angsuthanasombat, C., Keeratichamreon, S., Leetacheewa, S., Katzenmeier, G. and Panyim, S. (2001) Directed mutagenesis of the *Bacillus thuringiensis* Cry11A toxin reveals a crucial role in larvicidal activity of argining-136 in helix 4. J. Biochem. Mol. Biol. 34: 402-407.
- 1.2 Kanintronkul, Y., Sramala, I., Katzenmeier, G., Panyim, S. and Angsuthanasombat, C. (2003) Specific mutations within the α4-α5 loop of the *Bacillus thuringiensis* Cry4BA toxin reveals a crucial role for Asn-166 and Tyr-170. *Mol. Biotechnol.* 24: 11-19.
- 1.3 Puntheranurak, T., Uawithya, P., Potvin, L., Angsuthanasombat, C. and Schwartz, J.L. (2004) lon channels formed in planar lipid bilayers by the dipteran-specific Cry4B Bacillus thuringiensis toxin and its α1-α5 fragment. Mol. Membr. Biol. (in press).
- 1.4 Pornwiroon, W., Katzenmeier, G., Panyim, S. and Angsuthanasombat, C. (2004) Aromaticity of Tyr-202 in the α4-α5 loop is essential for toxicity of the Bacillus thuringiensis Cry4A toxin. J. Biochem. Mol. Biol. (accepted).
- 1.5 Angsuthanasombat, C., Uawithya, P., Leetachewa, S., Pornwiroon, W., Ounjai, P., Kerdcharoen, T., Katzenmeier, G. and Panyim, S. (2004) Bacillus thuringiensis Cry4A and Cry4B mosquito-larvicidal proteins: homology-based 3D model and implications for toxin activity. J. Biochem. Mol. Biol. (accepted).

2. International Meeting Abstracts

- Sramala, I., Sansom, M., Fischer, W., Katzenmeier, G., Panyim, S. and Angsuthanasombat, C.
 (2001) Molecular dynamics simulations of the transmembrane α4-α5 hairpin of the Bacillus thuringiensis Cry4B toxin. Biophys. J. 80; 297.
- 2.2 Sramala, I., Katzenmeier, G., Panyim, S. and Angsuthanasombat, C. (2002) Charged residues in helix 4 of the Bacillus thuringiensis Cry4B toxin are involved in ion channel activity: molecular dynamics simulation studies. In Abstract of the VIII International Colloquium on Invertebrate Pathology and Microbial Control, Foz do Iguassu, Brazil, p. 34.
- 2.3 Angsuthanasombat, C., Sramala, I., Puntheranurak, T., Kanintronkul, Y., Krittanai, C., Katzenmeier, G. and Panyim, S. (2002) Molecular basis of membrane pore-formation by the Bacillus thuringiensis Cry4B mosquito-larvicidal protein. In Abstract of the VIII International Colloquium on Invertebrate Pathology and Microbial Control, Foz do Iguassu, Brazil, p. 66.

The same of the sa

- 2.4 Puntheranurak, T., Potvin, L., Schwartz, J.L., Krittanai, C., Katzenmeier, G., Panyim, S. and Angsuthanasombat, C. (2002) Ion-channel activity of the Bacillus thuringiensis Cry4B α1-α5 pore-forming fragment. In Abstract of the VIII International Colloquium on Invertebrate Pathology and Microbial Control, Foz do Iguassu, Brazil, p. 53.
- 2.5 Kanintronkul, Y., Katzenmeier, G., Panyim, S. and Angsuthanasombat, C. (2002) Mutagenesis of α4-α5 loop residues in the pore-forming domain of the Bacillus thuringiensis Cry4B toxin. Biophys. J. 82: 559.
- 2.6 Pornwiroon, W., Katzenmeier, G., Panyim, S. and Angsuthanasombat, C. (2002) Mutations in α4 of the *Bacillus thuringiensis* Cry4A toxin reveal a critical residue for toxicity and ion channel activity. *Biophys. J.* 82: 558.
- Angsuthanasombat, C., Sramala, I., Puntheeranurak, T., Keeratichamreon, S., Krittanai, C., Katzenmeier, G. and Panyim, S. (2002) Molecular basis of the *Bacillus thuringiensis* toxininduced pore structure and permeability. *Biophys. J.* 82: 7.
- 2.8 Pornwiroon, W., Katzenmeier, G., Panyim, S. and Angsuthanasombat, C. (2003) A critical role in toxicity of two histidine residues in α4 of the Bacillus thuringiensis Cry4A toxin. Blophys. J. 83: 124.
- 2.9 Ounjai, P., Katzenmeier, G., Panyim, S. and Angsuthanasombat, C. (2003) Proline induced kink in α4 implies the importance of helix flexibility in the functional pore-formation of the Bacillus thuringiensis Cry4B toxin. Biophys. J. 83: 78.

3. Students Graduated in Ph.D. (Molecular Genetics and Genetic Engineering)

3.1 Name: Mr. Issara Sramala

Date of Graduation: 15 July 2002

Thesis Title: "Molecular Biophysical Studies of Transmembrane Helices in the Pore-Forming

Domain of the Bacillus thuringiensis Cry4B Toxin "

3.2 Name: Miss Theeraporn Puntheranurak

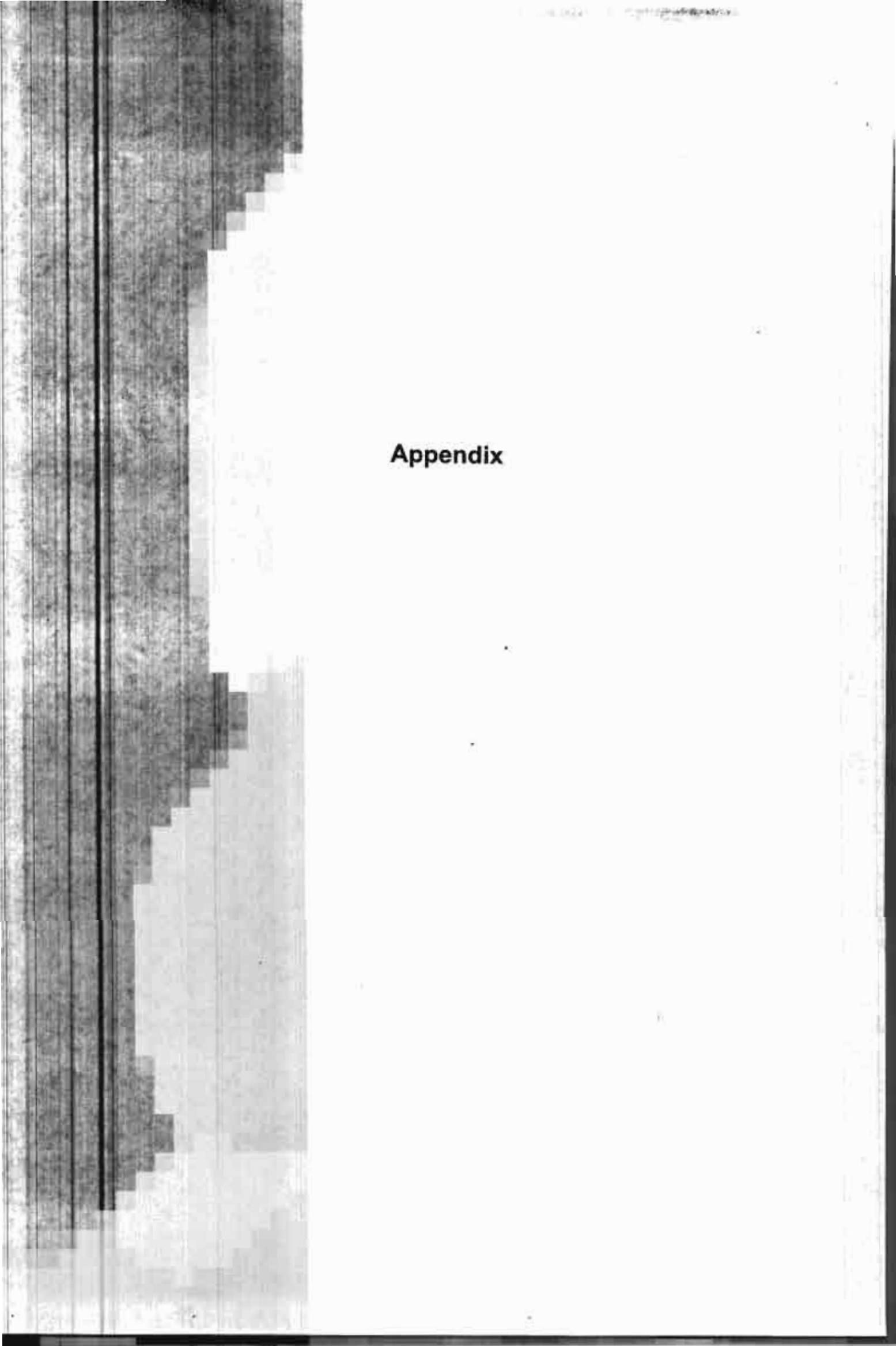
Date of Graduation: 16 May 2003

Thesis Title: * Structure-Activity Relationship Analysis of the Putative Pore-Forming Fragment of the Bacillus thuringiensis Cry4B δ-Endotoxin *

3.3 Name: Miss Walairat Pornwiroon

Date of Graduation: 28 November 2003

Thesis Title: "Mutational Analysis of Selected Residues in α4 and the α1-α5 Loop of the Bacillus thuringiensis Cry4Aa Toxin"



Directed Mutagenesis of the Bacillus thuringiensis Cry11A Toxin Reveals a Crucial Role in Larvicidal Activity of Arginine-136 in Helix 4

Chanan Angsuthanasombat*, Siriporn Keeratichamreon, Somphob Leetacheewa, Gerd Katzenmeier and Sakol Panyim

Laboratory of Molecular Biophysics. Institute of Molecular Biology and Genetics, Mahidol University, Salaya Campus. Nakompathom 73170, Thailand

Received 10 May 2001, Accepted 6 June 2001

Based on the currently proposed toxicity model for the different Bacillus thuringiensis Cry &-endotoxins, their pore-forming activity involves the insertion of the 04-05 helical hairpin into the membrane of the target midgut epithelial cell. In this study, a number of polar or charged residues in helix 4 within domain I of the 65-kDa dipteranactive Cry11A toxin, Lys-123, Tyr-125, Asn-128, Ser-130, Gln-135, Arg-136, Gln-139 and Glu-141, were initially substituted with alanine by using PCR-based directed mutagenesis. All mutant toxins were expressed as cytoplasmic inclusions in Escherichia coli upon induction with IPTG. Similar to the wild-type protoxin inclusion, the solubility of each mutant inclusion in the carbonate buffer, pH 9.0, was relatively low. When E. coli cells, expressing each of the mutant proteins, were tested for toxicity against Aedes aegypti mosquito-larvae, toxicity was completely abolished for the alanine substitution of arginine at position 136. However, mutations at the other positions still retained a high level of larvicidal activity. Interestingly, further analysis of this critical arginine residue by specific mutagenesis showed that conversions of arginine-136 to aspartate, glutamine, or even to the most conserved residue lysine, also abolished the wild-type activity. The results of this study revealed an important determinant in toxin function for the positively charged side chain of arginine-136 in helix 4 of the Cry11A toxin.

Keywords: Bacillus thuringiensis, δ-endotoxin, Inclusion solubility, Larvicidal activity, Site-directed mutagenesis

E-mail: stcas@mahidol.ac.th

Introduction

Bacillus thuringiensis (Bt), a Gram-positive endosporeforming bacterium, produces insecticidal proteins in large quantities as different forms of parasporal crystalline inclusions during sporulation (Hofte and Whiteley, 1989). These cytoplasmic inclusions are composed of one or several polypeptides that have been classified as Cry and/or Cyt δendotoxins on the basis of the similarity of their deduced amino acid sequences (Hofte and Whiteley, 1989; Crickmore et al., 1998). Currently, the Cry &-endotoxins have been shown to be active against insect larvae in the orders Diptera (mosquitoes and flies), Lepidoptera (moths and butterflies), Coleoptera (beetles and weevils), and Hymenoptera (wasps and bees) (Schnepf et al., 1998; de Maagd et al., 2001). For instance, the 65-kDa Cry11A toxin and the 130-kDa Cry4B toxin that are produced from Br subsp. israelensis are specifically toxic to mosquito larvae (Hofte and Whiteley, 1989; Schnepf et al., 1998).

The Bt &-endotoxins exist as inactive protoxins found within inclusion bodies, which require alkaline solubilisation and proteolytic activation in the insect larval midgut (Hofte and Whiteley, 1989). It has been proposed that, after activation by gut proteases, the active toxins kill the susceptible larvae via a two-step receptor mediated mechanism, in which the initial toxin-receptor interaction is followed by membrane insertion of the toxins to form transmembrane leakage pores. These pores cause the target midgut epithelial cells to swell and lyse by colloid-osmotic lysis (Knowles and Ellar, 1987), resulting in extensive damage to the midgut and eventually larval death (Knowles, 1994). However, the precise mechanism of action of the Bt toxins is still not completely understood, although knowledge of how these insecticidal proteins work at the molecular level has increased substantially over the last decade.

To date, the three-dimensional structures of two different Cry δ-endotoxins, Cry1Aa, and Cry3A have been solved by

^{*}To whom correspondence should be addressed. Tel: 662-441-9003, 1278; Fax: 662-441-9906

X-ray crystallography (Li, Carroll and Ellar, 1991; Grochulski et al., 1995). Both structures display a high degree of overall structural similarity and are composed of three structurally distinct domains. It is apparent that the N-terminal domain, a seven-helix bundle (six amphipathic helices around a central core helix), is clearly equipped for membrane insertion and pore formation (Li, Carroll and Ellar, 1991; Grochulski et al., 1995). This suggestion has been supported by various studies demonstrating that the isolated helical fragment from different Cry toxins is responsible for pore-forming activity (Walters et al., 1993; Von Tersch et al., 1994; Puntheeranurak et al., 2001).

The molecular mechanism of membrane insertion and pore formation of the Cry toxins is now described in an 'umbrella' model (Knowles, 1994). In this model, 0:4 and 0:5 form a helical hairpin to initiate membrane penetration upon specific receptor-binding in which structural rearrangement of the toxin occurs. After insertion of this hairpin, the other helices spread over the membrane surface followed by oligomerization of the toxin (Gazit et al., 1998; Guereca and Bravo, 1999), resulting in formation of an initial tetrameric pore (Schwartz et al., 1997). Currently, this model is supported by a number of experiments, which demonstrates the crucial role of 0x4 and 0x5 in pore-forming activity of different Cry toxins (Schwartz et al., 1997; Kumar and Aronson, 1999; Masson et al., 1999; Nunes-Valdes et al., 2001). Recent studies clearly demonstrated that the helix 4loop-helix 5 hairpin is more active in membrane penetration than each of the isolated helices, or their mixtures, consistent with its function as the membrane-inserted portion of the Cry toxins (Gerber and Shai, 2000).

In earlier studies, we demonstrated that α4 and α5 of the 130-kDa Cry4B toxin are essential determinants of toxicity, likely to be involved in pore formation rather than in receptor recognition (Uawithya et al., 1998; Sramala et al., 2000). In addition, arginine-158 in helix 4 was found to play an important role in larvicidal activity of this toxin (Sramala et al., 2001). In the present report, an analogous effect on toxicity was observed for the 65-kDa dipteran-specific Cry11A toxin when charged, and polar residues in helix 4 were altered. The results revealed that the specific structure for the positively charged side chain of arginine-136 in this helix is directly involved in Cry11A toxin activity, supporting the notion that α4 is essential for pore formation by the Cry δ-endotoxins.

Materials and Methods

Plumids and site-directed mutagenesis. The full-length gene, encoding the 65-kDa Cry11A toxin from the recombinant plasmid pBTC68A (a generous gift of Dr. Wattanalai Panbangred, Department of Biotechnology, Mahidol University, Thailand), was subcloned into the pMEx8 expression vector (Buttcher et al., 1990). This resultant plasmid (pME4D) was used as a template for site-directed mutagenesis. Each complementary pair of mutagenic oligonocleotide primers was purchased from Genset Inc.

Table 1. Complementary primers for substituting a coded residue with different amino acids.

Primer		Sequence*	Restriction Site	
#1238-F		CTOCHOGTTATTTTCTAAATC	3* Pal	
F1214-F	E-CATTERCAL	MATANC CTOCACCTGTTGCAC	730	
******	B 441111440	CONTINUE CHICAGO CITOTIOCAL		
	G A	LIGALFO	7	
M134M-1	2 01001001	TANTAC AMBETTACCTCANT	TTG 3' //indill	
HT18W-E	3 CANATIGNO	OCTA ANDCYTOTATTATAGENC	CAC 3	
	1 0	RLPQTAV	0 T	
T-ALPIZ	5 TAATACAM	GTCTACCTCAATTTGCAGTTC	AAACAT 3'Acci	
E141A-E	5 ATOTTON	C TOCAATTGAGGTAGACGT	GTATTA 3'	
	LHL	8 G A I I O M	1	
R136K-E	5 CTAARTOTA	MOT GODOCCATAATACAAAA	STROCTC 3" Heefill	
R136K-F	5 GAGGTAAT	TTTGTATTAT GCCCCACTT	C SKTTAG	
	LHL	5 6 A 1 1 0 0	L P	
R136Q-f	5 CTAMATCTI	MOT GOTOCCATAATACAA CAA	TTACCTC 3" AMIV	
K1360-L	S'GAGGTAAT	POTTGTATTAT GOCACCACTTA	GATTING 3	
	G A 1	1 9 B L 7 9 F		
#136D-E	5'GGTGCTNT	MINCA MEATETROCTCANTTY	GAGG 3" Belli	
#136D-F		CAGGE ASSECT TOTATTATAL		
	LSG		0.7	
Q135A-2	S'CTANGTOC	TGCCATAATAGCTAGGTTACCT	CARTTEG 1' BUILL & AM	
Q135A-E	35A-1 S'CAAATTGA GETAACCTAGCTATTATGGCACCACTTAG 3'		CACTTAG 1	
			•	
Q139A-E		CANCETCTACCTCCTTTTCAC		
Q139A-F	5"GAACCTCA	U. MCCAGOTMGACGTTGTATTA	TACC 1	
A. same			THUC 9	
077-740		EGAPLHL	and an area of	
T1258-E	P. CANCAGCCI	AAGGGTWCCTTTCTAAATCTAA	G 3" MMV	
1135A-E	5 CTTAGATTT	AGANA GOCACCCTTGGCTGTT	e 3.	
		LALSC		
H128A-f		TCTA OCATTRAGTOGTGC 3"		
H128A-E	5°GCACCACT1	A ATOCTAGAAAATAACCC 3		
5139A-5		TARATCT GGCCGGTGCTATAA		
\$130A-F	S'GTATTATAG	CACC GOCCAGATTTAGAAAAT	MAC 3"	

Introduced restriction enzyme recognition sites are underfined. The mutated nucleotide residues are shown as boldface. Deduced amino acid sequences are shown on top of each pair of oligonucleotide primers.

(Singapore), as shown in Table 1. All mutations were generated by PCR using high fidelity *Pfu* DNA polymerase following the procedure of the QuickChange^{1M} mutagenesis kit (Stratagene). All mutant plasmids were analyzed by DNA sequencing using a Perkin Elmer ABI prism 377 automated sequencer.

Toxin expression and characterization. The wild type and mutant Cry11A toxin genes were expressed in the E.coli strain JM109 under control of the inducible tac promoter. Cells were grown in a LB medium that was supplemented with 100 μg ml ampicillin until OD_{um} reached 0.4-0.5. Incubation was continued for another 4 h after addition of isopropyl-β-D-thiogalacto-pyranoside (IPTG) to the final concentration of 0.1 mM. Protein expression was analyzed by sodium dodecyl sulfate (SDS)-15% w/v polyacrylamide gel electrophoresis (PAGE). Immunoblotting was performed with polyclonal rabbit antibodies against the Cry11A toxin (kindly provided by Prof. David Ellar, University of Cambridge, UK). Immunocomplexes were detected with an antirabbit antibody-alkaline phosphatase conjugate (Sigma).

E. coli cultures, expressing each mutant as cytoplasmic inclusion bodies, were harvested by centrifugation, resuspended in distilled

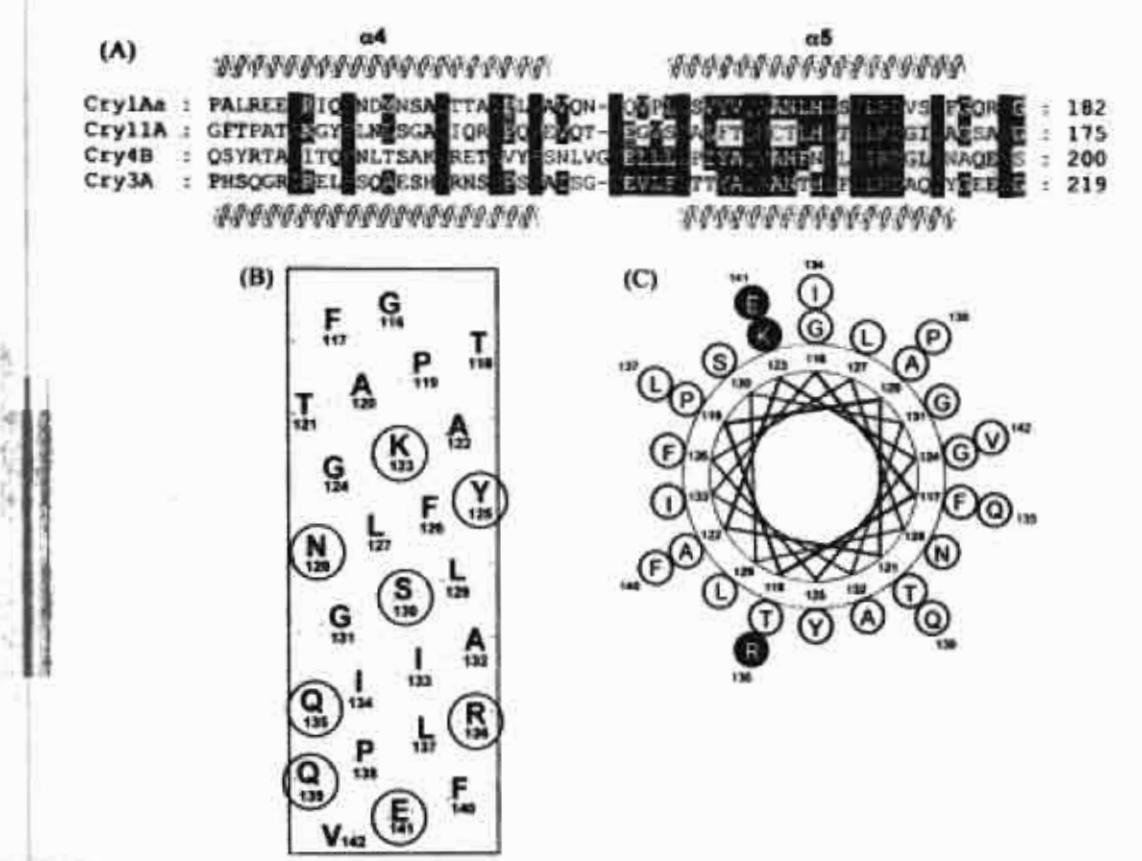


Fig. I. (A) Multiple sequence alignment of helices 4 and 5 of Cry11A with the crystal structures of Cry1Aa and Cry3A, and the homology-based model of Cry4B. The sequences were aligned using the program CLUSTAL W. The degree of conservation is represented by background shading of the residues with the darkest shading for the most conserved: 100% conserved, 75% conserved, and 50% conserved. The positions of secondary structure elements of Cry1Aa and Cry3A are illustrated over and under the alignments, respectively. (B) The predicted pattern of helix 4 of Cry11A is composed of 27 residues of which the encircled residues were mutated. (C) A helical wheel projection of helix 4 of Cry11A. Amino acid residues are plotted every 100 degrees consecutively around the wheel, following the sequences given in B. The following color code is used: black is an amino acid with a charged side chain, gray is a polar side chain, and white is a hydrophobic side chain.

water, and disrupted in a French Pressure Cell at 16,000 psi. The crude lysates were centrifuged at 8,000 g for 5 min and the pellets obtained were washed 3 times in distilled water. Protein concentrations were determined by using a protein microassay (Bio-Rad) with the bovine serum albumin fraction V (Sigma) as a standard. Protoxin inclusions (1 mg ml⁻¹) were solubilized in 50 mM Na₂CO₂ pH 9.0 and incubated at 37°C for 60 min, as described previously (Uawithya et al., 1998). After centrifugation for 10 min, the supernatants were analyzed by SDS-PAGE in comparison with the inclusion suspension.

Larvicidal activity assays Bioassays were performed, as described previously (Angsuthanasombat et al., 1993), using 2-day old Aedes aegypti mosquito-larvae reared from eggs that were supplied by the mosquito-rearing facility of the Institute of Molecular Biology and Genetics, Mahidol University, Thailand. About 500 larvae were reared in a container (22 × 30 × 10 cm) with approximately 3 litres of distilled water that was supplemented with a small amount of rat diet pellets. Both rearing and bioassays were performed at room temperature (25°C). The assays were carried out in 1 ml of E. coli suspension (10° cells suspended in distilled water) in a 48-well micrometer plate (11.3 mm well diameter) with 10

larvae per well and a total of 100 larvae for each type of *E. coli* samples. *E. coli* cells, containing the recombinant plasmid pME4D and the pMEx8 vector, were used as positive and negative controls, respectively. Mortality was recorded after a 24-hour incubation period.

Results and Discussion

Based on a multiple-amino acid sequence alignment with the known crystal structures of Cry1Aa and Cry3A (Li, Carroll, and Ellar, 1991; Grochulski et al., 1995), and the homology-based model of Cry4B (Uawithya et al., 1999), the predicted α4 and α5 were located within the pore-forming domain of Cry11A (see Fig. 1A). Charged amino acids in helix 4 were shown to be critical for toxin activity (Kumar and Aronson, 1999; Masson et al., 1999; Sramala et al., 2001). To investigate the possible role for toxicity of charged and polar amino acids in α4 of Cry11A, a PCR-based mutagenesis strategy, previously employed for Cry4B (Sramala et al., 2001), was applied to obtain substitutions within Cry11A. We initially generated eight Cry11A mutants in which three